

Life Cycle Assessment

*Thermal Energy Storage Systems Using Recycled Steel
Industry Waste for Concentrated Solar Power Plants*

Master's Thesis for the degree of

Master of Science (M.Sc.)

University Koblenz - Landau

Zentrum für Fernstudien und universitäre Weiterbildung

Energiemanagement

Yvonne Bäuerle

(Basel, Switzerland)

Koblenz, 2017

Life Cycle Assessment

*Thermal Energy Storage Systems Using Recycled Steel
Industry Waste for Concentrated Solar Power Plants*

Master's Thesis for the degree of

Master of Science (M.Sc.)

University Koblenz - Landau

Zentrum für Fernstudien und universitäre Weiterbildung

Energiemanagement

30 October 2017

Author: Yvonne Bäuerle, born on 14 October 1983

Supervisor: Christian Bauer, Paul Scherrer Institut, CH-Villigen

Co-supervisor: Prof. Ralf Antes, ZFUW, Koblenz-Landau

ACKNOWLEDGEMENT

First of all, I would like to thank my supervisor, Christian Bauer, and co-supervisor, Prof. Ralf Antes, for their expertise, ideas, feedback, time, and encouragement.

Special thanks go to Dr. Christian Wieckert for giving me this great opportunity to conduct my Master Thesis within the Slagstock project at the Paul Scherrer Institute (PSI). He always had an open door and the profitable discussions and support in every aspect of the project was essential for the successful completion of this work.

I am also very grateful to all Slagstock partners for their close collaboration with me on this project. In particular, the valuable communication efforts of Dr. Javier Rodríguez, Dr. Erika Garitaonandia, and Patrick Boucharinc tremendously contributed to the success of the LCA.

Additionally, I would like to thank Giuseppe Casubolo and Ana Maria Barraza from SQM for their cooperation by providing detailed information and data on the manufacturing process of the solar salt; this was very helpful and it significantly improved the scientific insights of the LCA.

Thanks and recognition also goes to Andrea Ulitzsch for her administrative support from the ZFUW.

Last, but not least, I would like to thank my beloved husband, Greg Stechishin, for his moral support, reviewing efforts, and understanding.

TABLE OF CONTENTS

Abstract	i
1 Introduction	1
2 Concentrated solar power electricity generation	5
2.1 CSP technology	8
2.2 Thermal energy storage systems	12
2.2.1 Two-tank TES system	16
2.2.2 Single-tank thermocline TES system	18
2.3 Sensible heat storage material production	21
2.3.1 Mined solar salt	22
2.3.2 EAF slag filler material	24
3 Life cycle assessment methodology	29
3.1 Goal and scope definition	29
3.2 Life cycle inventory	30
3.3 Impact assessment	30
3.4 Interpretation	31
4 Description of EAF slag-based storage systems studied	33
5 Inventory collection	40
5.1 Thermocline storage tank	40
5.2 Mined solar salt	42
5.3 EAF slag filler material	43
5.4 Alternative TES system comparison	44
5.5 50 MWe molten solar salt CSP central receiver plant including EAF slag-based TES system	45
6 Results	47
6.1 Mined solar salt	48
6.2 EAF slag filler material	49

6.3 Embodied life-cycle GHG emissions by TES systems	50
6.4 50 MWe CSP central receiver plant including EAF slag-based TES system	55
7 Summary and Conclusions	58
References.....	61
Appendix A: List of Figures.....	ii
Appendix B: List of Tables	v
Appendix C: List of Abbreviations	vi
Appendix D: LCI datacollection for TES systems 1 – 5	vii
Appendix E: LCI datacollection for CSP components	xv
Appendix F: CSP Scaling functions.....	xix
Appendix G: LCI datacollection Solar Salt	xxii
Appendix H: Declaration / Erklärung	xxiii

ABSTRACT

A comparative life cycle assessment (LCA) was performed to evaluate a thermal energy storage system (TES) using electric arc furnace (EAF) slag in a packed bed storage configuration against other commonly used molten solar salt-based TES options for application in concentrating solar power (CSP) plants. TES systems are designed for six hours of thermal storage when implemented in 50 MWe CSP plants. The environmental performance is quantified and discussed with a focus on life-cycle greenhouse gas (GHG) emissions. Other selected performance indicators are provided, as well.

This Master's Thesis is part of the joint European Slagstock project which studies the use of EAF slag as a filler material in a thermocline (one tank) TES system design. In this project, two pathways to produce the EAF slag pebble filler material from raw EAF slag are investigated: a sintering method and a mechanical conformation process.

This LCA evaluates in more detail the implementation of an EAF slag-based thermocline TES system in CSP tower plants that use mined molten solar salt as a heat transfer fluid (HTF). The analysis indicates that switching from a commonly used direct two-tank configuration to the EAF slag thermocline TES configuration reduces TES related life-cycle GHG emissions by 38% when the pebbles are produced via the sintering method and 58% via mechanical conformation, respectively.

Further, future CSP technologies using air as an HTF in the implementation of the EAF slag thermocline TES designs are estimated to improve life-cycle GHG emissions by 53 – 55% in comparison to molten solar salt-based EAF slag thermocline TES systems.

Finally, a common molten solar salt-based CSP tower plant integrating a thermocline TES system with mechanical conformed EAF slag pebbles located in Seville, Spain, is also compared against other renewable and non-renewable electricity generation to be used for Spanish electricity supply. Over its life cycle, this CSP configuration is estimated to generate life-cycle GHG emissions of 27.7 gCO_{2eq}/kWh_e, which is very significantly lower (by approx. 97%) when compared to life-cycle GHG emissions from natural gas or coal generation. Overall, most environmental performance indicators of solar thermal electricity production are comparable to wind turbine technology.

1 INTRODUCTION

Solar thermal electricity (STE) generation from concentrated solar power (CSP) plants is a commercially proven technology. The recent IEA roadmap (IEA, 2014) envisions a continuous growth of STE production over the next few decades to a share of up to 11% of the total electricity generation, leading to an installed CSP capacity of 1000 gigawatt (GW) by 2050. Achieving this vision would reduce annual carbon dioxide (CO₂) emissions by up to 2.1 gigatonnes (Gt) making cleaner electricity generation possible.

A major benefit of the CSP technology is the option to operate the solar power plant in conjunction with large thermal energy storage (TES) systems, thus enabling stable and dispatchable¹ power delivery. This allows for reliable electricity generation from CSP plants and provides the ability to shift electricity generation to meet different profile needs. For example, excessive solar heat (depending on the solar irradiance) can be stored in the TES system during daytime and released on demand to produce electricity when sunshine is not available.

Comparing CSP applications (including long term storage systems) to other renewable technologies, like photovoltaic (PV) or wind reveals a better potential for dispatchability and for operating as a baseload facility by providing round the clock electricity generation. These characteristics are the main benefits of STE among other renewable electricity generation methods. As an example, thermal storage has been applied in 40% of Spanish CSP plants since 2010, delivering an average of five to ten hours storage. The IEA noted, “when thermal storage is used to increase the capacity factor², it can reduce the levelised cost of STE.” (IEA, 2014). New developments of CSP plants today always incorporate energy storage because CSP is only including TES systems competitive and complementary to PV.

Consequently, TES systems play a crucial role in CSP applications, not only because it is easier to store the energy in a large scale in form of heat rather than electricity, but also because it is more affordable. Furthermore, common TES

¹ Dispatchable power delivery is the ability of a plant to provide electricity on the operator's demand.

² The capacity factor is the amount of electricity produced in a year (GWhe) divided by the product of nominal capacity of the plant (MWe) multiplied by the number of hours in a year (8760 hours).

technologies still show the potential to further increase their efficiency and cost-effectiveness, which is a key for future CSP developments (Gil, et al., 2010).

The most common TES systems used in commercialized solar thermal power plants are making use of sensible heat storage³ by applying a heat transfer fluid (HTF) as a direct or indirect⁴ storage medium. State-of-the art, utility-scale CSP plants featuring several hour TES systems like the Gemasolar plant, a 19.9 MWe CSP tower plant (Burgaleta, Arias, & Ramirez, 2011), use molten “solar salt”⁵ both as an HTF and a liquid sensible heat storage material due to its superior heat-transfer and energy-storage capabilities.

However, using molten salt requires thousands of tons for a large scale application (e.g., 28'500 tons in the 50MWe ANDASOL 1 plant in Granada, Spain) and leads to several drawbacks, such as the limited operation temperature range (220 – 565°C), the worldwide availability of salts, and their high cost.

An alternative HTF in a CSP central receiver application can be air, which allows to reach higher operation temperatures (550 – 1000°C) when implemented in an open volumetric air receiver⁶ design (Hennecke, et al., 2008). This concept was tested at Jülich's 1.5 MWe Solar Power Tower, a first-of-its kind demonstration plant in Germany to serve as a reference for future commercial systems.

Currently, R&D activities on thermal storage systems evaluate sensible heat, latent heat⁷, and chemical energy⁸ pathways where the focus of the research is on finding materials and methods that allow for better thermodynamic behavior and improved chemical compatibility (Bauer, et al., 2017).

Although latent heat storage provides a few advantages over sensible heat storage, the technological and economical aspects of sensible heat storage make it a

³ The heat is stored by increasing the temperature of the storage material in an insulated vessel.

⁴ Solar thermal energy in a direct TES system is stored in the same fluid used to collect it. Different fluids are used as the heat-transfer and storage fluids in an indirect TES application as described in 2.2.1.

⁵ Standard „solar salt” consists of a mixture of 60wt% NaNO₃ and 40wt% KNO₃. It has a melting point of 220°C and starts to decompose above 565°C.

⁶ Open volumetric air receivers absorb the heat from concentrated sunlight and transfer it to the air which is sucked through its porous structure.

⁷ Latent heat storage systems store the energy in phase change materials (e.g. from solid to the liquid phase).

⁸ Thermochemical storage allows for chemical reactions.

superior option (Singh, Saini, & Saini, 2010). One way to further improve common sensible storage technology and make it more cost-effective is to partially replace the relative costly molten solar salt utilized as the storage medium. A packed bed thermal storage system configuration is an attractive option in this case.

The packed bed consists of a suitable filler material providing good thermodynamic properties when in direct contact with the HTF in an insulated vessel. With respect to materials that are required for high temperature (120 – 1400°C) energy storage, Hasnaina (1998) mentions that the literature proposes inorganic salts, metals or solid industrial waste as storage material (e.g. solid industrial wastes like copper slag, iron slag, cast iron slag, aluminum slag, and copper chips).

Iron and steel slags are a non-metal, rock-like by-product in the steel making industry and are naturally separated from the liquid metal when heating scrap steel, iron, lime, or coke beyond their melting point. Specifically electric arc furnace (EAF) slag is produced during the manufacturing of crude steel from metal scrap and currently only partially recycled in several applications such as aggregates for construction or road materials. This slag is produced approximately 40 Mt per year worldwide and only around 2.9 million tons (Mt) of EAF steel slag are still landfilled per year in Europe (EUROSLAG – The European Slag Association, 2017).

EAF slag as a filler material to obtain a low-cost storage material appears to be a promising alternative and might improve current TES systems considerably. Its utilization could open up new possibilities within the framework of CSP and would lead to a cost-effective high temperature storage solution for both current and future TES applications. Additionally, an EAF slag-based TES system could be easily applied in future CSP systems using air as an HTF.

Nevertheless, when evaluating new technologies and more efficient and cost-effective solutions, such as an EAF slag-based TES system, we also have to factor in the environmental sustainability and their contribution to greenhouse-gas (GHG) emissions and other environmental burdens. The potential advantages of the newly developed systems need to be demonstrated from an environmental perspective. A standardized procedure to evaluate this is a life cycle assessment (LCA) which determines the environmental impact associated with a product from resource extraction to end-of-life burdens. The assessment also includes an interpretation and acknowledgement of the system components and the needs for improvement, especially when compared to other technologies.

This Master's Thesis evaluates the environmental "footprint" of an innovative EAF steel slag-based TES system and investigates all stages of it from cradle-to-grave, factoring in both system configurations using molten solar salt or air as an HTF. The LCA is part of the SOLAR-ERA.NET project Slagstock (Table 1) and delivers an analysis and comparison of the environmental impact of the proposed TES system for the application in CSP plants. The international Slagstock research team developed a 500 kWh pilot plant at the CIC energiGUNE research center (work package, WP 4) to evaluate the technical feasibility and deliver important design conclusions. However, the technical and economical assessment (TEA), WP 5 and the LCA (WP 6) are carried out at a utility-scale for an easier comparison to currently applied systems.

Table 1: Slagstock major Work Packages and participants; Coordinator: CIC energiGUNE. Further partner: University Erlangen / Nuremberg.

Slagstock major Work Packages and participants; Coordinator: CIC energiGUNE	LEADER	TYPE	COUNTRY
1 - Definition of the TES system parameters for CSP applications and characterization of steel slag	IK4-Azterlan	Research Center	Spain
2 - Modelling of the TES system	CIC energiGUNE	Research Center	Spain
3 - Manufacture of the EAF slag filler material	Tellus Ceram	SME	France
4 - Testing of the TES pilot plant	CIC energiGUNE	Research Center	Spain
5 - Technical and Economical Assessment (TEA)	ArcelorMittal S.A.	Large Enterprise	Spain
6 - Life Cycle Assessment (LCA) of the new TES systems	PSI	Research Center	Switzerland

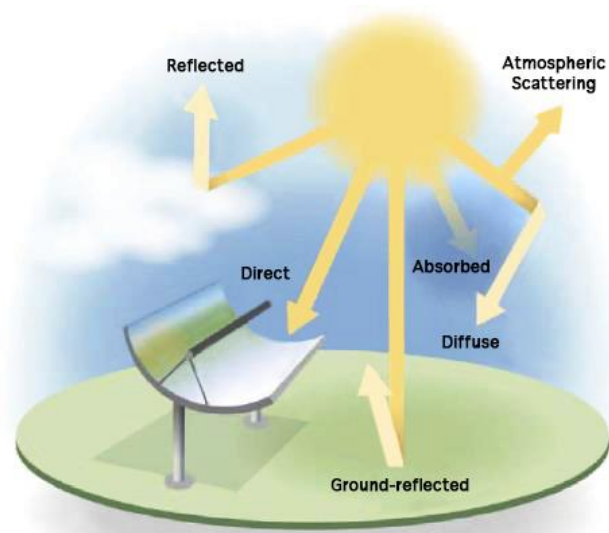
By factoring in the defined TES system parameters (WP 1) and applying thermodynamic modeling (WP2) for a 50 megawatt (MWe) CSP plant, the design settings (e.g. vessel size, filler material mass, etc.) of the EAF slag-based TES system were established.

2 CONCENTRATED SOLAR POWER ELECTRICITY GENERATION

Harnessing solar energy to generate electricity is achieved by concentrating solar radiation via reflective mirrors to produce temperatures high enough to drive heat engines. Parabolic shaped reflectors, as illustrated in Figure 1, concentrate the sunlight on a focal line or focal point where the heat is absorbed in a receiver system.

Sunlight consists of direct and indirect components. Indirect radiation can be defined as diffused light which is reflected and scattered, whereas direct radiation⁹ reaches the Earth's surface directly (i.e. DNI or Direct Normal Irradiance).

Figure 1: Concentrating solar technology can only use part of the solar radiation, the direct irradiation. Parabolic shaped mirrors focus this light creating high temperatures which can be used to drive a steam engine.



Unlike solar photovoltaics (PV) which use both, direct and diffuse solar irradiance, only direct irradiation is suitable to be concentrated and transferred in a receiver system which provides thermal energy to a conventional steam cycle for electricity generation.

⁹ Radiant energy can be measured in joules, though it is more commonly measured as radiant flux, or radiant power, which is expressed as energy over time. The sun emits 3.846×10^{26} W. The energy that reaches Earth is measured as solar irradiance (energy per second over a square meter). Given the estimated radiant power of the sun, the intensity of solar energy that reaches the top of Earth's atmosphere (directly facing the sun) is $1'360 \text{ W/m}^2$ (Fondriest Environmental, Inc., 2017).

For this reason, CSP plants can provide cost-effective energy specifically in regions with DNI > 2'000 kilowatt hour of direct radiation per square meter annually ($\text{kWh/m}^2/\text{year}$), typically found in the so called Sunbelt regions (Middle East and North Africa, South Africa, the southwestern United States, Mexico, Chile, Peru, Australia, India, western China, southern Europe and Turkey) where some of the best sites receive more than 2'800 $\text{kWh/m}^2/\text{year}$. In this case, one square kilometre of land can annually generate as much as 100 – 130 GWhe of STE from CSP facilities.

At the end of 2015, the worldwide operational STE capacity reached 4.9 GW with an annual electricity production of 15 TWhe (Teske, 2016). This still makes up only a small fraction of the reported CSP global technical potential of almost 30'000'000 TWhe (Trieb, et al., 2009) required to meet the global electricity demand of currently 21'191 TWhe.

The GHG emission reduction is the most important environmental benefit from solar energy generation. Greenhouse gas (GHG) emissions from STE are much lower compared to fossil fuel driven electricity technologies with CSP plants already now reducing CO_2 equivalent ($\text{CO}_{2\text{eq}}$) emissions ranging from 5'760 – 14'505 t $\text{CO}_{2\text{eq}}/\text{year}$. The level of CO_2 emissions lowered by STE depends upon the fuel or combination of fuels that the solar electricity is displacing (Bauer, et al., 2017).

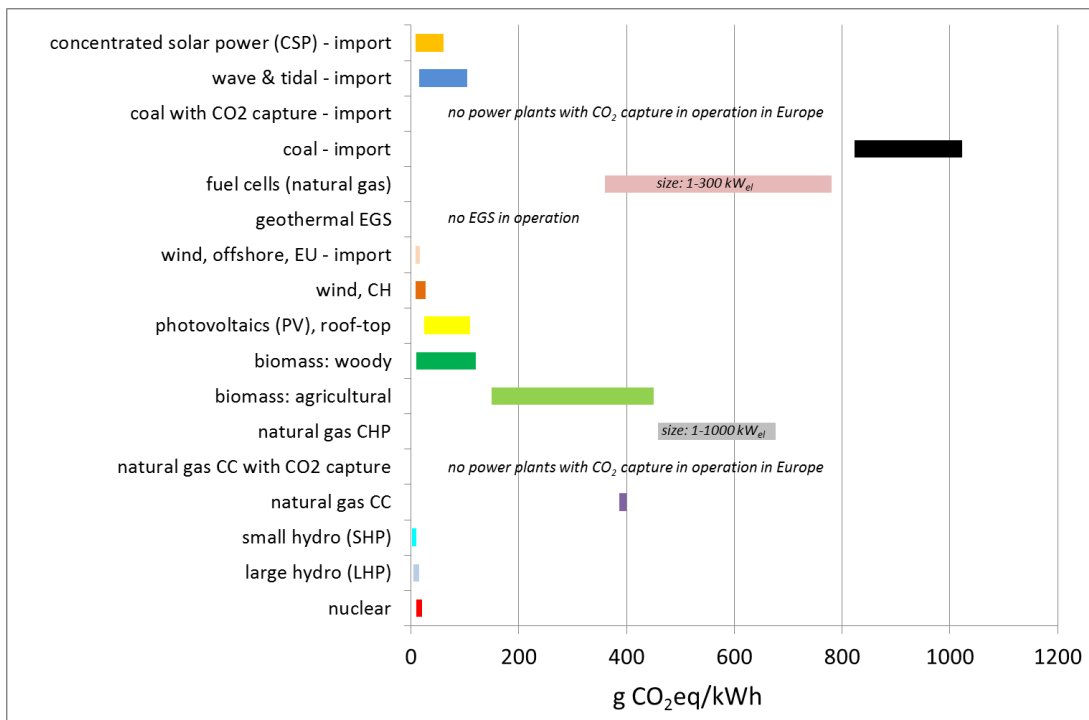
The environmental impact of STE generation highly depends on the technology, system configurations, and the type of operation. CSP plants generally consist of a solar field for harnessing the solar energy, an energy back-up system and a power block which runs a conventional steam power cycle to generate electricity.

Figure 2 shows an overview of the life cycle GHG emissions of current electricity generation technologies, where the presented results from STE production are retrieved from Burkhardt, et al. (2012). These values present a “harmonized” (variability reduction by using consistent plant design and performance parameters, global warming intensities, and system boundaries) environmental impact ranging from 5 – 60 g $\text{CO}_{2\text{eq}}/\text{kWhe}$ for solar only TES components.

Some operational CSP plants do not entirely run on solar-only resources and feature a fossil fuel back-up system which generates thermal energy at times when there is not enough solar heat available. These integrated, solar combined cycle or hybrid plants combine CSP and fossil fuel co-firing. CSP plants with a natural gas boiler as a back-up system have 4 – 9 times more life cycle GHG emissions than plants with non-hybrid TES systems (Klein & Rubin, 2013).

Therefore, the integration of long term TES systems into CSP plants as an alternative to hybrid CSP systems is preferable from an environmental point of view.

Figure 2: Life cycle GHG emissions of current electricity generation technologies (at the power plant¹⁰). Ranges reflect variability in terms of site-conditions, technology specification, and fuel characteristics. Combined heat and power generation in CHP units and fuel cells is allocated according to exergy content of heat and electricity. Data availability for biomass is limited. NG: natural gas; CC: combined cycle; CHP: combined heat and power; LHP: large hydropower; SHP: small hydropower; CSP: concentrated solar power; PV: photovoltaics; EGS: enhanced geothermal systems; CCS: carbon capture and storage; “coal” includes hard coal and lignite. (Bauer, et al., 2017)



For example, the 110 MWe Atacama STE plant (central receiver system) in Chile, currently under construction, will cover 17.5 hours of thermal storage (molten solar salt), and, therefore, be able to produce solar-only electricity 24 hours a day basically every day of the year. In order to be able to charge the TES system while producing electricity at the same time, the thermal capacity of the collector field has to provide excessive heat. The relation between the heat capacity from the solar field at the receiver (\dot{Q}_{SF}) and the thermal requirement of the steam cycle (\dot{Q}_{SC}) is called the Solar Multiple (SM).

$$Solar\ Multiple = \frac{\dot{Q}_{SF}}{\dot{Q}_{SC}}$$

¹⁰ Electricity transmission and distribution is not accounted for.

A CSP system configuration with an SM of two, for example, consists of a solar field twice the size of that which is required to deliver thermal energy to cover just the steam power cycle capacity. The additional excessive heat from the solar field can be used to charge the storage system and, when there is no solar irradiance available anymore, the discharge of the storage system provides the required thermal energy to continue the electricity production.

For a CSP plant to be able to deliver reliable and dispatchable power delivery, the capacity and dimensions of the TES system plays a decisive role. With respect to capacity, it is necessary to configure the SM based on the location, respectively the DNI and the electricity delivery requirements.

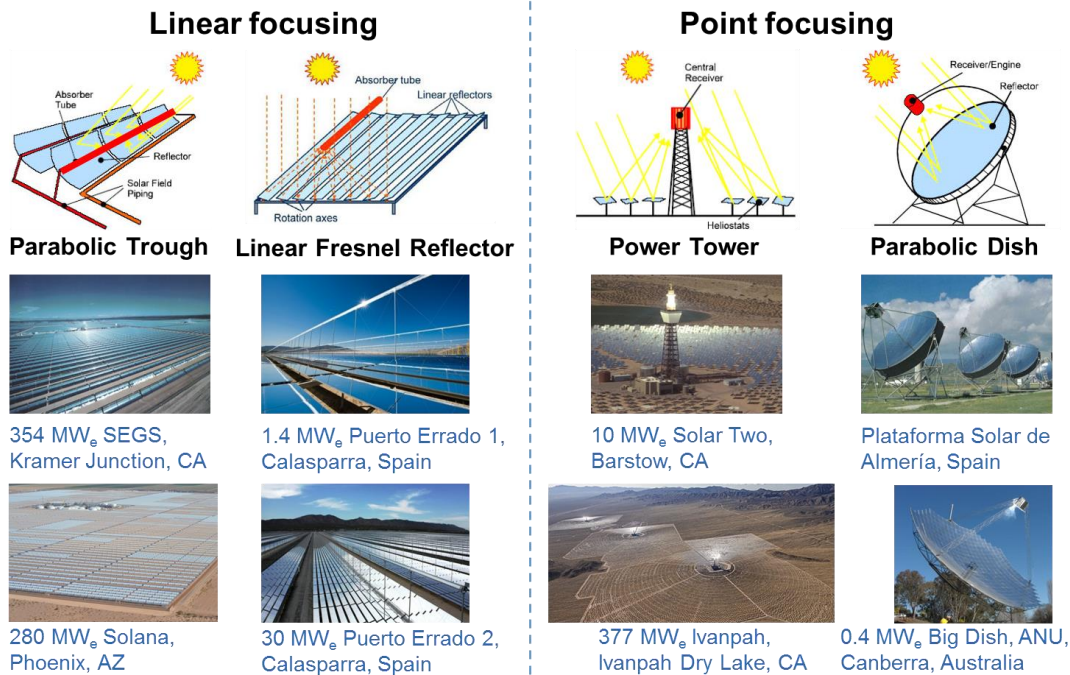
This LCA focuses on a CSP solar-only operation modus, therefore life-cycle GHG emissions per unit output (kWh_e) of the investigated CSP plant including the EAF slag-based TES system are expected to stay within the range of the proposed 5 – 60 g CO_{2eq}/kWh_e.

2.1 CSP technology

There are four main types of CSP technologies: parabolic troughs, linear Fresnel, central receivers, parabolic dishes. Line concentrating plants are designed using parabolic trough and linear Fresnel systems, whereas parabolic dishes and central receivers are used in point concentrating central receiver systems, with the latter also known as solar towers (Figure 3). Parabolic dishes are more suitable for decentralized applications since the typical size of a single parabolic dish module is 10 kWh_e to 25 kWh_e and they are individually driven by a Stirling engine allowing flexible and independent operation, while the other CSP technologies are mostly used for centralized electricity production.

Figure 3: Schematics of CSP Technologies (SolarPACES 2016a). Examples of commercial parabolic troughs are the 354 MWe SEGS¹¹ plants in California (constructed in 1985-91) and the 280 MW Solana plant in Arizona (2013); Fresnel reflector systems are operational in Spain as 1.4 MW prototype (2009) and 30 MW commercial plant (2012); Solar power towers have been built in California as 10 MW prototype (1996) and 377 MW commercial plant (2013); Parabolic dish prototypes with Stirling engines are being tested in Spain (25 kW modules constructed in 1996-97) and Australia (400 kW big dish erected in 2011) (Bauer, et al., 2017).

Concentrating Solar Power (CSP) Technologies



Currently, the parabolic trough system is the most mature and commercially proven CSP technology (20 years of operating experience), reaching a share of up to 80% of today's globally installed capacity (4.9 GWe). This system features absorber tubes, where concentrated sunlight (70 - 80 times the nominal value) heats up synthetic thermal oil to a maximum of 400°C, a limit dictated by its chemical properties. The thermal oil is then pumped through a heat exchanger producing slightly superheated steam at high pressure which is fed into a steam turbine connected to a generator to produce electricity. Recent developments replace the synthetic thermal oil with direct steam or molten solar salt to increase solar-to-electricity efficiency, such as the 5 MWe Archimede parabolic trough plant in Italy.

Linear Fresnel reflector systems use almost flat mirrors installed in long rows to reflect direct sunlight onto a fixed secondary concentrator receiver located above

¹¹ SEGS – Solar Electricity Generation System.

the receiver tube. These reflectors track the sun independently and the fixed absorber tube allows for easier direct steam generation (DSG), and, therefore, higher temperatures. However, optical losses are greater compared to trough plants leading to a reduced solar-to-electricity efficiency. Today, several 50 MWe Fresnel projects are under development¹² to further improve their technological maturity.

Central Receiver plants feature a circular array of heliostats (large mirrors with sun-tracking motion) reflecting direct sunlight onto an absorber system mounted on the top of a tower. Depending on the absorber design and its associated choice of HTF (e.g. water/steam, molten solar salt or a gaseous medium like air), maximum temperatures can principally reach up to 1'000°C. The higher temperatures lead to the production of superheated steam for the turbine, and, therefore, increase solar-to-electricity efficiency when operated via a steam engine cycle.

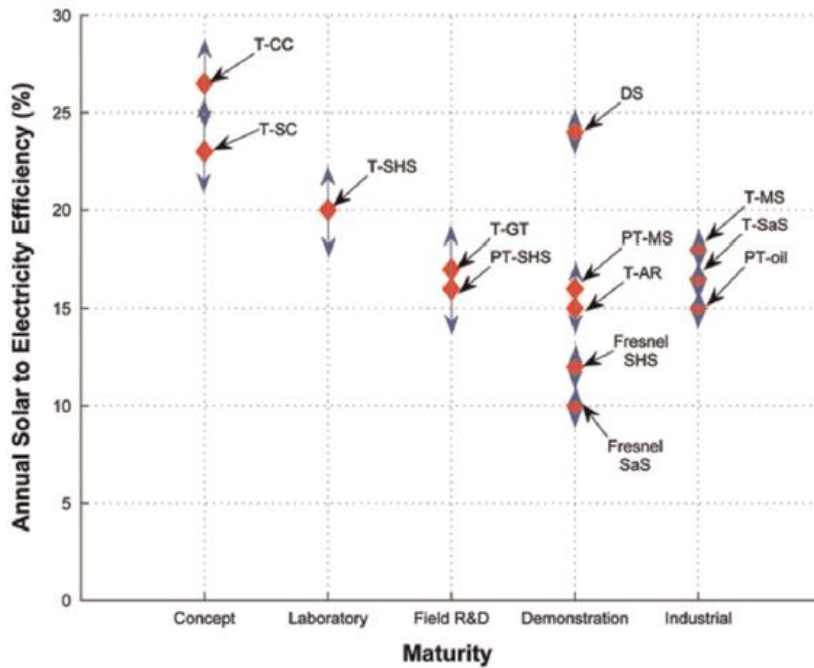
An open volumetric receiver plant uses ambient pressure air and a modular ceramic receiver design to drive a steam Rankine cycle (Hennecke, et al., 2008). R&D also focuses on pressurized volumetric air receiver designs which could potentially replace natural gas in a gas turbine. In general, central receiver systems are offer the largest prospects for future cost reductions. Nevertheless, the development of high temperature receivers that operate with large temperature ranges (RT¹³ – 1'000°C) is still in the early stages of development with fundamental challenges which have been observed being related to materials durability and reliability.

Figure 4 provides an overview over expected efficienciess (i.e. the ratio of electricity generated to the solar energy input) and maturity levels of major process options.

¹² NREL, https://www.nrel.gov/csp/solarpaces/linear_fresnel.cfm

¹³ Room temperature

Figure 4: Annual solar-to-electricity efficiency as a function of development level for each CSP technology family (European Academies Science Advisory Council, easac, 2011).



CSP technology	Technical options
Parabolic troughs (PT)	PT-oil: oil as HTF and molten salt storage PT-SHS: superheated steam as HTF PT-MS: molten salt as HTF and storage
Linear Fresnel systems (F)	Fresnel SaS: saturated steam as HTF Fresnel SHS: superheated steam as HTF
Towers (T)	T-SaS: saturated steam as HTF T-SHS: superheated steam as HTF T-MS: molten salt as HTF and storage T-AR: ambient pressure air as HTF and Rankine cycle T-GT: pressurised air as HTF and Brayton cycle T-SC: supercritical cycle T-CC: pressurised air as HTF and combined cycle
Parabolic dishes (DS)	DS: helium Stirling cycle

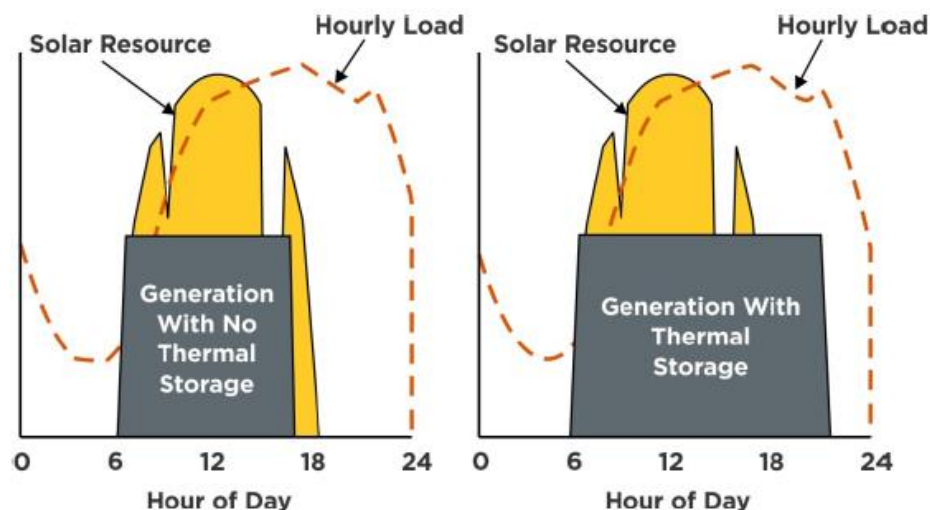
Central receiver plants using molten solar salt as both an HTF and a storage material, such as the 110 MWe Crescent Dunes STE plant with an incorporated 10 hours thermal storage unit (also known as direct thermal storage systems), have an improved temperature range (290 – 565°C) and subsequently expanded thermal energy capacity. As a result, they require less storage material in comparison to parabolic trough systems using thermal oil as an HTF (290 – 390°C). This also leads to a simplified system design that further improves costs as there is no need for an additional heat exchanger.

The concepts of thermal storage systems are discussed in the following section.

2.2 Thermal energy storage systems

Integrating a TES system into a CSP plant enables the ability to generate electricity beyond the daytime sun hours. This allows for greater utilization of the power block, thus increasing the capacity factor, and potentially reducing levelised costs of solar thermal electricity (LCOE). The increased electricity output overcomes the investment of the required, larger solar field and the TES system, thereby maximizing value to the utility and revenue to the owner (Figure 5). In the case of CSP solar-only operation with no storage, the capacity factor is directly related to the site dependent available solar irradiation.

Figure 5: Thermal storage and utility demand. STE production with solar-only operation and no thermal storage option show the same characteristics as photovoltaic and wind energy generation, which highly depend on the renewable energy resource. Adding a thermal storage component to a CSP plant allows for extending and/or shifting energy generation to match with peak load demands.



Source: NREL

To effectively store heat, three components are typically required: a storage medium with good thermo-physical characteristics, an efficient heat transfer mechanism, and a suitable containment system. As described before, the heat can be stored in the form of sensible heat, latent heat which uses phase change materials (PCM), or reversible chemical reactions. Today, the most common TES systems used in commercialized solar thermal power plants are based on molten solar salt (sensible storage) as an indirect or direct implementation in a two-tank configuration (Kuravi, et al. , 2013). Nevertheless, systems utilizing latent heat, thermochemical, and other sensible heat materials are in development. “With respect to performance, the key differentiating characteristics of the wide array of TES media that have been

developed over the years are operating temperature range, gravimetric and volumetric storage density¹⁴, and cost.” (Siegel, 2012).

However, the TES component costs of the complete CSP system design is an additionally factor and storage medium cost savings might be off-set by additional costs of the heat transfer mechanism or container system. Moreover, the system performance of the storage component is also influenced by its application properties and operation requirements. Therefore, in order to evaluate the economic and environmental impact of a given TES strategy, a CSP system level analysis is necessary.

For example, in a study on solid media direct thermal energy storage for CSP parabolic trough applications using thermal oil as HTF, Laing, et al. (2006) investigated whether concrete and castable ceramic are suitable as a sensible heat storage material. Experiments on a 350 kWh pilot setup, performed at temperatures up to 325°C, show high suitability of the realized system. The advantage of the concrete storage concept is the low cost of the storage medium, however, the heat capacity is lower compared to other options, and, therefore, requires larger volumes, increasing the costs of the heat exchangers and engineering (Kuravi, et al., 2012).

Table 2 presents storage material candidates for the various storage mechanisms and their thermo-physical properties over a temperature range of 350°C. Research efforts on TES systems applicable to CSP plants are reviewed in Kuravi, et al. (2013) with the suggestion that researchers should put emphasis on the exergetic efficiencies in the design of storage systems to reduce their costs while moving towards higher temperatures. Experiments to improve the solar salt mixture using calcium nitrate, or lithium nitrate reveal difficulties due to decomposition at temperatures above 460 – 550°C. Compatibility tests regarding a suitable sensible heat filler material in a nitrate salt system show that some natural minerals are more suitable than others. For example, quartzite rock, aluminum oxide, and iron ore pellets show very good compatibility with molten nitrate salts, when bauxite, limestone, and marble did not prove to be suitable. Some recent research projects, including the Slagstock project, evaluate sensible storage materials based on industrial wastes as a storage filler material (Calvet, et al., 2013), (Ortega, et al., 2014).

¹⁴ Gravimetric storage density (kJ/kg) and volumetric storage density (MJ/m³) are two thermo-physical properties which provide information about the amount of thermal energy stored in a material with respect to its mass or volume.

Table 2: Physical properties of selected thermal energy storage media. Sensible energy storage media, both liquid and solid, are assumed to have a storage temperature differential of 350°C with respect to the calculation of volumetric and gravimetric storage density (Siegel, 2012).

Storage Medium	Specific Heat (kJ/kg-K)	Latent or Reaction Heat (kJ/kg)	Density (kg/m ³)	Temperature Range (°C)		Gravimetric Storage Density (kJ/kg)	Volumetry Storage Density (MJ/m ³)
				Cold	Hot		
Sensible Energy Storage—Solids							
Concrete	0.9	–	2200	200	400	315	693
Sintered bauxite particles	1.1	–	2000	400	1000	385	770
NaCl	0.9	–	2160	200	500	315	680
Cast iron	0.6	–	7200	200	400	210	1512
Cast steel	0.6	–	7800	200	700	210	1638
Silica fire bricks	1	–	1820	200	700	350	637
Magnesia fire bricks	1.2	–	3000	200	1200	420	1260
Graphite	1.9	–	1700	500	850	665	1131
Aluminum oxide	1.3	–	4000	200	700	455	1820
Slag	0.84	–	2700	200	700	294	794
Sensible Energy Storage—Liquids							
Nitrate salts (ex. KNO ₃ -0.46NaNO ₃)	1.6	–	1815	300	600	560	1016
Therminol VP-1 [®]	2.5	–	750	300	400	875	656
Silicone oil	2.1	–	900	300	400	735	662
Carbonate salts	1.8	–	2100	450	850	630	1323
Caloria HT-43 [®]	2.8	–	690	150	316	980	676
Sodium liquid metal	1.3	–	960	316	700	455	437
Na-0.79K metal eutectic	1.1	–	900	300	700	385	347
Hydroxide salts (ex. NaOH)	2.1	–	1700	350	1100	735	1250
Latent Energy Storage							
Aluminum	1.2	397	2380	–	660	397	945
Aluminum alloys (ex. Al-0.13Si)	1.5	515	2250	–	579	515	1159
Copper alloys (ex. Cu-0.29Si)	–	196	7090	–	803	196	1390
Carbonate salts (ex. Li ₂ CO ₃)	–	607	2200	–	726	607	1335
Nitrate salts (ex. KNO ₃ -0.46NaNO ₃)	1.5	100	1950	–	222	100	195
Bromide salts (ex. KBr)	0.53	215	2400	–	730	215	516
Chloride salts (ex. NaCl)	1.1	481	2170	–	801	481	1044
Flouride salts (ex. LiF)	2.4	1044	2200	–	842	1044	2297
Lithium hydride	8.04	2582	790	–	683	2582	2040
Hydroxide salts (ex. NaOH)	1.47	160	2070	–	320	160	331
Thermochemical Energy Storage							
SO ₃ (g) ↔ SO ₂ (s) + 1/2O ₂ (g)	–	1225	–	–	650	1225	–
CaCO ₃ (s) ↔ CO ₂ (g) + CaO(s)	–	1757	–	–	527	1757	–
CH ₄ (g) + CO ₂ (g) ↔ 2CO(g) + 2H ₂ (g)	–	4100	–	–	538	4100	–
CH ₄ (g) + H ₂ O(g) ↔ 3H ₂ (g) + CO(g)	–	6064	–	–	538	6064	–
Ca(OH) ₂ (s) ↔ CaO(s) + H ₂ O(g)	–	1351	–	–	521	1351	–
NH ₃ (g) ↔ 1/2N ₂ (g) + 3/2H ₂ (g)	–	3900	–	–	195	3900	–

Experiments on PCM for high temperature storage applications using molten carbonates report difficulties regarding the compatibility with the containment material. Only a mix of barium carbonate and sodium carbonate show stable performance and good compatibility. Routes to incorporate PCM thermal storage into CSP applications can be realized via a heat exchanger system which requires

high level engineering or by encapsulation of the PCM within a coating and using it as a filler material in a packed bed system (Muñoz-Sánchez, et al., 2015).

Nevertheless, applicability of PCM into CSP plants for high temperature materials still needs to be investigated (Kuravi, et al., 2013).

In the literature, most results of environmental assessments on high temperature TES systems for CSP plants available are based on complete CSP plant evaluations using common utility-scale, molten solar salt, two-tank implementations (Heath, et al., 2009), (Whitaker, et al., 2013), (Lechon, et al., 2008), (Telsnig, 2015). Their results highly depend on the temperature range, system size, system boundaries, operation conditions, and their CSP implementation (global warming potential, (GWP) from the TES component varies from 0.4 – 14.6 gCO_{2eq}/kWh). In order to truly compare life cycle GHG emissions from various TES systems, the system boundaries should therefore be similar.

Heath, et al. (2009) compares the embodied life cycle GHG emissions of an indirect two-tank storage system to a theoretical thermocline single tank storage system. Both TES systems are molten solar salt based with 6 hours of thermal capacity for 50 MWe CSP parabolic trough applications. Results show that a thermocline, silica sand packed bed design reduces GHG emissions more than 50%. This can be associated to the lower solar salt inventory and the simplification of the system design.

On the other hand, Oro, et al. (2012) compares the “global impact”¹⁵ of three different TES system designs:

- 350 kWht indirect TES system using a concrete-based heat exchanger design for common thermal oil CSP parabolic trough applications (120 - 390°C).
- 600 MWht direct two-tank molten solar salt TES system for CSP tower applications (290 – 550°C).
- 100 kWht PCM – TES system based on nitrate salt for direct steam CSP applications (195 – 235°C).

Results show that the global impact of the concrete-based TES system is the lowest (0.01 Impact/kWht), followed by the molten solar salt design (0.47 Impact/kWht),

¹⁵ The global impact category is based on the Eco-Indicator 99 (EI99) impact assessment method which combines the environmental burdens: human health, ecosystem quality, and resources.

and finally the PCM-TES system (1.12 Impact/kWh). The results on the climate change (GWP), however, are not provided. Nevertheless, the comparative LCA of two TES systems in “Sham 1 CSP plant: molten salt vs. concrete” from Adeoye et al. (2014) concludes that a concrete TES system shows a greater GHG emissions than a conventional molten solar salt TES system.

Lalau, et al. (2016) investigates the environmental impact of an industrial waste-based TES system. The study evaluates an alternative ceramic filler material using Cofalit (manufactured from asbestos recycled waste) for a molten solar salt thermocline tank TES design. The results compare the direct application of this alternative system to a common indirect, two-tank TES system (7.5 hours) for a utility-scale 50 MWe CSP parabolic trough plant. The conclusion from this study is similar to the one in Heath, et al. (2009): The GWP of the alternative thermocline TES system (2.4 gCO_{2eq}/kWh) is lower in comparison to the conventional two-tank TES system (4.0 gCO_{2eq}/kWh). Nonetheless, the investigation raises the concern that not enough Cofalit could be provided for the expected TES material requirements and the suggestion to use fly ash or metallurgic slag instead was put forward.

The following sections explain in further detail the commonly used two-tank TES system design and the alternative thermocline storage system.

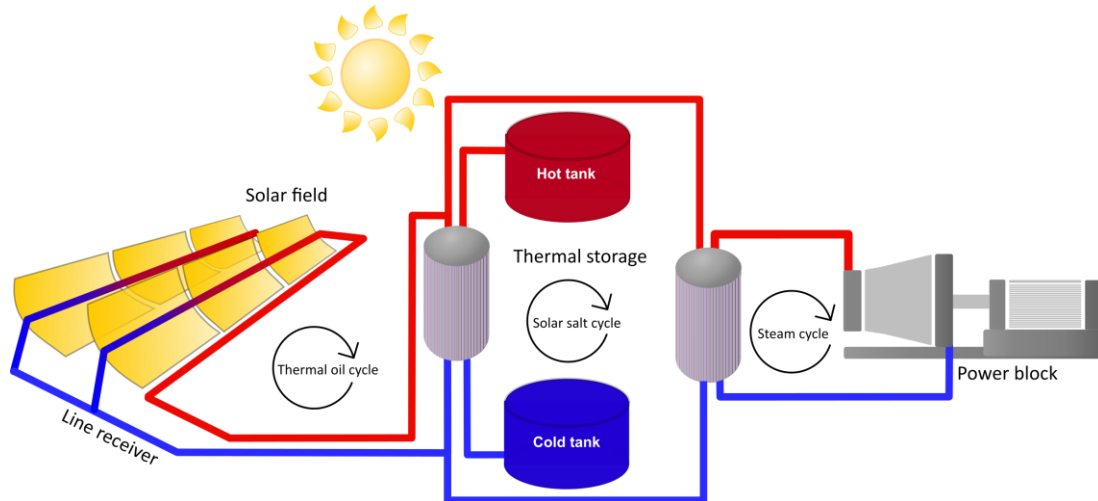
2.2.1 Two-tank TES system

At times when there is enough solar energy available, an HTF provides additional thermal energy from the solar field to charge an insulated tank (hot tank). For this reason, the TES system has to accommodate the extra mass of the HTF which is realized using a separate second tank (cold tank). This additional HTF is then pumped from the cold tank via the heat source into the hot tank during the charging cycle of the TES system. However, when there is heat demand from the steam cycle at times with little or no solar energy available, the HTF in the hot tank is discharged via the heat sink to the cold tank.

Two-tank molten solar salt TES systems can also be characterized as being either indirect or direct system designs. A schematic of the indirect approach is shown in Figure 6. In most cases, indirect TES systems are incorporated in CSP parabolic plants due to the high freezing point of molten solar salt (approximately 200°C) and its potential to freeze in the extensive piping with the solar field. This leads to significant operation and maintenance (O&M) challenges and the requirement for freezing protection, such as auxiliary heater systems (Kearney, et al., 2003).

For this reason, an additional heat exchanger is implemented in the TES system, enabling the separation of the HTF circulating in the collector field and the molten solar salt circulating between the storage tanks. This approach can therefore use an HTF in the collector field with a lower freezing point (12 – 390°C), typically synthetic oil, also known as thermal oil.

Figure 6: Parabolic trough CSP plant incorporating an indirect molten solar salt storage system.



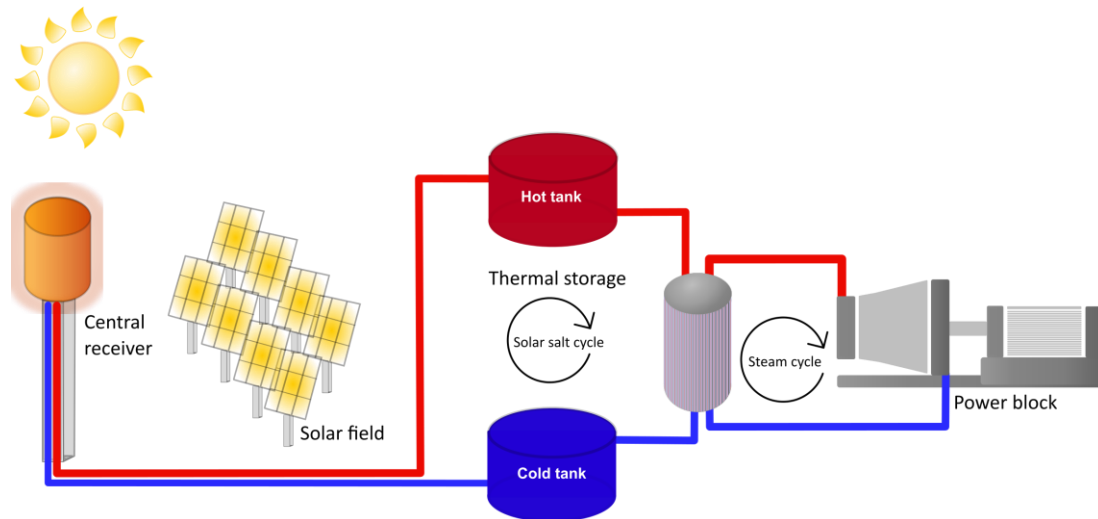
However, the use of thermal oil as a *storage media* in large quantities is difficult due to its high vapor pressure (>1 MPa at 400°C). “Multiple thick-walled pressure-vessels would have to be used to store the hot oil, which would be too costly to be practical.” (Pacheco, Showalter, & Kolb, 2002). Although higher HTF operating temperatures are desired in order to achieve higher efficiencies (Yang & Garimella, 2010), the indirect approach of separating the thermal oil and the molten solar salt via a heat exchanger is most feasible in this case.

A second heat exchanger or steam generator is placed between the steam Rankine cycle and the thermal oil cycle which finally provides superheated steam at nominal conditions of 377°C and 100 bar. A typical thermal storage efficiency for an indirect molten solar salt two-tank system in a parabolic trough application is about 93% and about 37% for the steam cycle (Libby & Key, 2009).

The direct approach to store thermal energy using molten solar salt (Figure 7) can, however, reach efficiencies up to 99%. This is due to the fact that the molten solar salt is heated up to higher temperatures (565°C) and is used as both, an HTF and storage media, which eliminates the need for a second set of heat exchangers used to transfer thermal energy between the HTF and the storage medium in the indirect system.

This approach is more commonly incorporated into central receiver plants because the application provides easier handling of the freezing challenges when installing an electric heat trace system (expected heat trace parasitic energy consumption is less than 1.5% of the total gross electricity production).

Figure 7: Central receiver CSP plant incorporating a direct molten solar salt storage system.



In this type of installation, the molten solar salt is pumped from the cold storage tank (290°C) through the receiver system directly into the hot storage tank (565°C). To provide thermal energy to the steam Rankine cycle, the hot molten solar salt is then discharged from the hot tank via the steam generator to create high-pressure superheated steam into the cold storage tank. However, the direct TES system does not require a fully charged TES system before it is able to run the steam Rankine cycle, which means that both storage tanks are able to hold the complete inventory of the molten solar salt. The HTF is recirculated and reused throughout the 30+ years of plant operation with no expected loss and can be recycled as fertilizer at the end of the CSP plants lifetime (Pacheco J. E., 2002).

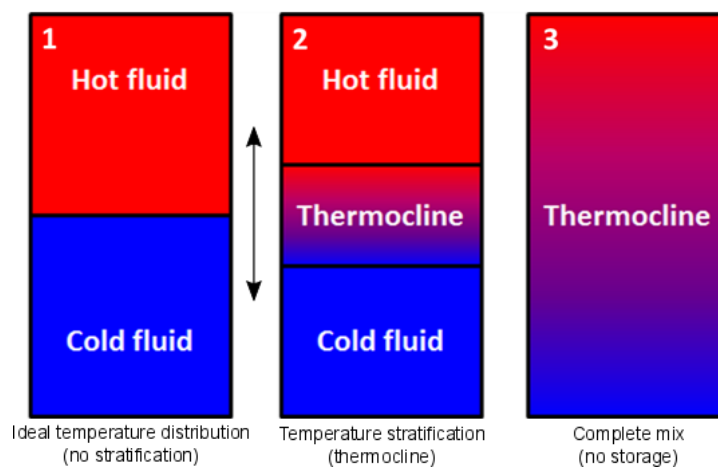
Still, a single-tank thermocline storage system with a low-cost filler material compared to a two-tank configuration is a more economically feasible option (Chang et al. 2014) and can also operate via a direct or indirect approach.

2.2.2 Single-tank thermocline TES system

In a single-tank thermocline TES system, a section with higher temperatures forms at the top of the tank during charging and is separated by a thermocline layer (due

to the buoyancy force¹⁶) from a colder section at the bottom of the tank (Figure 8). This thermocline layer moves up and down during charging and discharging. Ideally, the temperature stratification is minimal in order to achieve maximum storage capacity. In contrast, a complete mix of the hot and the cold fluid inside the tank, the temperature gradient between the hot and cold ends of the tank is negligible, leading to almost no storage effect.

Figure 8: Single-tank thermocline TES system. Ideal temperature distribution with no temperature stratification (1) leads to a maximum storage capacity. More realistically, temperature stratification (thermocline layer) forms between the hot and cold section (2). In case of a complete mix and temperature equalization in the tank there is no thermal storage effect (3).



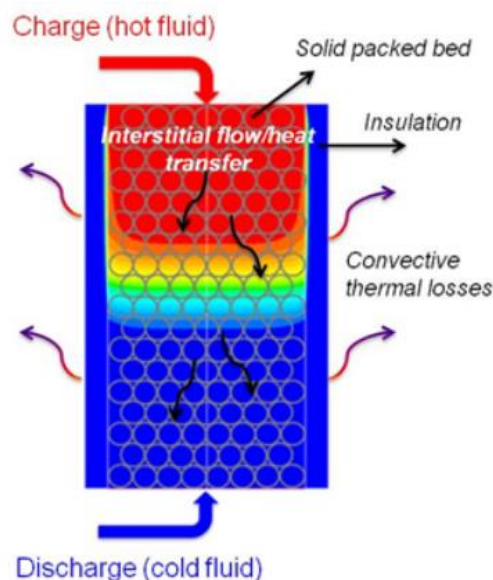
Additionally, a low-cost filler material with good thermo-physical characteristics is used to pack the tank volume, allowing the partial displacement of the molten solar salt (HTF), and acts as a primary packed bed storage medium. Due to the simpler system design (tank construction, pumps, valves, and piping) of the thermocline storage systems and the lower amount of needed HTF, cost reductions are as high as 35% in comparison to the two-tank TES systems (Brosseau, Hlava, & Kelly, 2005).

When the packed bed thermocline tank is charged, the cold fluid at the bottom of the tank is pumped either through the solar receiver system (direct) or the additional heat exchanger (indirect), depending on the TES system incorporated in the CSP plant, where it is heated up before it is fed into the top of the tank. Then the hot fluid

¹⁶ The upward force a fluid exerts on an object less dense than itself. Moreover the same volume of a hot fluid is lighter than cold fluid because of the hot fluids lighter density characteristic.

flows down through the porous bed, transferring the heat to the solid media (Figure 9). To discharge the system, the fluid flow is reversed.

Figure 9: Principle scheme of a thermocline packed bed configuration. A low-cost filler material forms a packed bed inside the tank, and, therefore, allows for the partial replacement of the HTF. The thermocline storage system is charged from the top of the tank, providing fluid flow through the porous bed and the transfer of heat to the filler material. In order to discharge the thermocline system, the fluid flow is reversed.



It is worth noting that experiments on packed bed thermocline storage systems have identified thermal ratcheting at the walls resulting from settling of the filler material during repeated thermal cycling. To avoid a failure of the thermocline tank without incurring excessive energy loss, the insulation between the steel shell and the filler region should be maximized (Flueckiger, Yang, & Garimella, 2011). Ideally, the thermal ratcheting should be examined as part of a detailed design process before large scale systems are developed (Libby, 2010).

In 2001, Sandia National Laboratories tested quartzite rock and sand as a filler material in a 2.3 MWh thermocline molten solar salt storage facility. The thermocline concept showed promising results, though additional studies were recommended, especially for applications above 400°C (Brosseau, Hlava, & Kelly, 2005) to further evaluate material durability and reliability.

Current research projects, like the Slagstock project, further investigate the thermocline thermal storage concept by developing numerical modelling (Flueckiger, et al., 2011), (Zanganeh, et al., 2012), (Modi & Perez-Segarra, 2014), (Mira-Hernandez, et al., 2015), (Chang, et al., 2015), (Ortega-Fernandez, et al., 2016) and by setting up test facilities for molten solar salt storage and component tests

(Sallaberry, et al., 2015), (Breidenbach, et al., 2016), (Fasquelle, et al., 2017) in order to evaluate other low-cost storage materials, and system integration for full commercial applicability.

Another advantage of the thermocline storage concept is its compatibility with the next generation CSP plants, where it can be directly integrated using air as an HTF. An example of such integration can be seen at the Jülich 1.5 MWe Solar Power Tower.

The focus of the research and development activities in the Slagstock project is on the evaluation of a packed bed thermocline storage system using molten solar salt or air as a HTF and EAF slag as a filler material. This thermocline concept is demonstrated and tested with air as an HTF in a 500 kWh pilot plant using a 100 kWe electric air heater system and a tank volume of one cubic meter containing 2'160 kg of EAF slag pebbles (10 mm spheres), leading to a void fraction¹⁷ of about 37%.

The following section describes the production methods of the storage materials required for the thermocline EAF slag-based packed bed TES system studied in the Slagstock project.

2.3 Sensible heat storage material production

The required storage materials for the investigated TES system are solar salt (HTF) and EAF slag pebbles (filler material in the thermocline tank).

The solar salt compounds, sodium nitrate and potassium nitrate, can be either produced via mining of natural resources or synthetically via a chemical reactions using nitric acid. Considering that nitric acid has an overwhelming GHG contribution from its production process and the large amount of solar salt needed in a TES system, it is obvious that the choice of the solar salt production has a significant effect on the life cycle impacts of the TES system. For example, Whitaker, et al. (2013) evaluates the environmental impact of a 106 MWe CSP tower plant using mined solar salt in comparison to synthetic salt (among other design alternatives). This study estimated an increase of GHG emissions by 12% when using a synthetic salt, stressing the importance of the storage material being studied in an LCA.

¹⁷ Large randomly packed beds of uniform spheres tend to pack with an average void fraction of 39%.

In order to determine the type of solar salt commonly used in industry, some CSP experts were consulted (Wieckert, 2017), revealing that, up to now, only mined solar salts are used in utility-scale CSP plants. Approximately 85% of global sodium nitrate production is supplied by natural deposits, the majority of which is located in Chile with Sociedad Quimica y Minera de Chile S.A. (SQM) being one of the largest mining operator. SQM also produces mined solar salt and was therefore chosen as the solar salt supplier in this LCA.

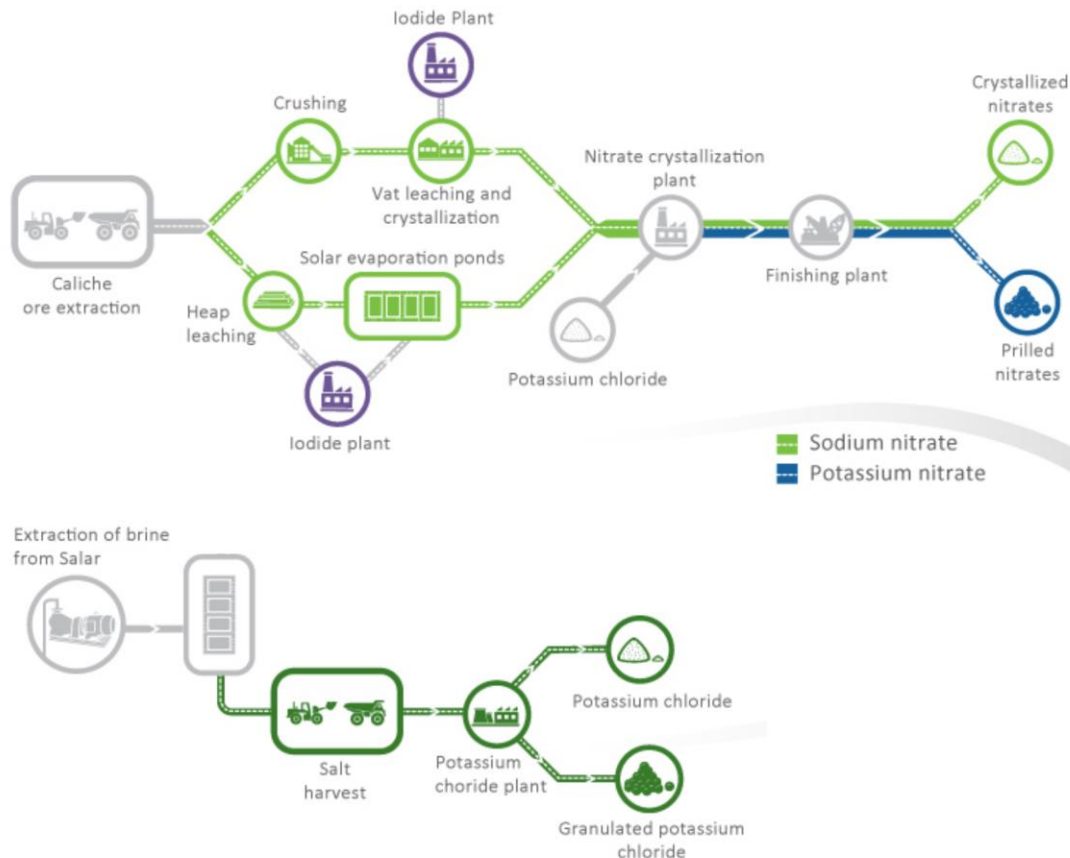
As for its inventory and its environmental impact, literature research across several LCAs on CSP technologies revealed a number of inconsistent assumptions which can be traced to a lack of data. It was therefore decided, that this LCA also investigates the production of solar salt in more detail.

2.3.1 Mined solar salt

The largest natural accumulation of sodium nitrate in mineral deposits can be found in the Atacama Desert in northern Chile as a result of its unique arid climate going back to the middle Miocene epoch. These mineral deposits, called “caliche ore”, are mined for the production of sodium nitrate and iodine, which are mainly produced by SQM via the closed-circuit Guggenheim method (Kogel, et al., 2006). At the same time, this region is rich in Salar brines which are formed through a natural leaching process in underground halite aquifers where increasing concentrations of lithium and potassium from the Andes Mountains are accumulated (Houston, et al., 2011).

Figure 10 illustrates the SQM mining and manufacturing process of the solar salt. The caliche ore can be mined from seams that are between 0.2 and 5 m thick on the surface under a layer of overburden material (0.5 – 1.5 m) using drilling machines, explosives, and bulldozers, etc. Sodium nitrate can then be dissolved after further crushing of the caliche ore (about 12 mm in diameter) and the application of a heated leaching process in big vats (at about 40°C). The leaching solution is mainly composed of the mother liquor from the nitrate crystallization process, weak brines generated in the washing stages of the leaching cycle, and fresh water. Depending on the material composition of the caliche ore and the desired material component outputs, it can also be processed using heap leaching (without crushing) and solar drying in large evaporation ponds. The product from the leaching is then sent to the crystallization process. After dry harvesting, the nitrate salts are used in the production of potassium nitrate.

Figure 10: Process flow diagram of the mining solar salt production at SQM in northern Chile (Atacama Desert). Solar salt is produced using two natural resources, Caliche Ore and Salar brines. After extraction of the raw material, leaching and several crystallization processes form sodium and potassium nitrates. Controlled forming of potassium nitrate is established via the following chemical reaction: $\text{NaNO}_3 + \text{KCl} = \text{KNO}_3 + \text{NaCl}$. An additional final crystallization process then leads to the favorable mix of the solar salt (60 wt% sodium nitrate and 40 wt% potassium nitrate). (SQM, 2017)



Salar brines, on the other hand, are pumped via standard wells from approximately 0.5 – 30 m below a salt crust into large evaporation ponds (plastic-lined) to concentrate the salts. This site in the Atacama Desert is best suited for solar drying (8 – 10 months) as shown in Figure 11, since it offers very dry atmospheric conditions. The initial phase chemistry is controlled by mixing brines from separate evaporation ponds to remove the magnesium and sulfate at the early stages of the evaporation. The salts rich in potassium chloride can be harvested by excavators.

Both harvested salts (sodium nitrate and potassium chloride) are transported via trucks and trains to the nitrate processing plant where two further crystallization processes at moderate temperatures (40°C and 80°C) are performed. The chemical production process of potassium nitrates (KNO_3) is formed via sodium nitrate (NaNO_3)

extracted from the caliche ore and potassium chloride (KCl) harvested from the Salar brines.

Figure 11: Production facilities for the manufacturing process of solar salt in the Atacama Desert, Chile. In (a), the caliche ore extraction is illustrated and (b) shows the evaporation ponds and harvested salt piles from the salar brine. Illustration (c) shows the process plant for the nitrate production. (SQM, 2016)

Caliche ore surface mining (a)



Salar Brine evaporation ponds and harvesting (b)



Processing plant for nitrate production (c)

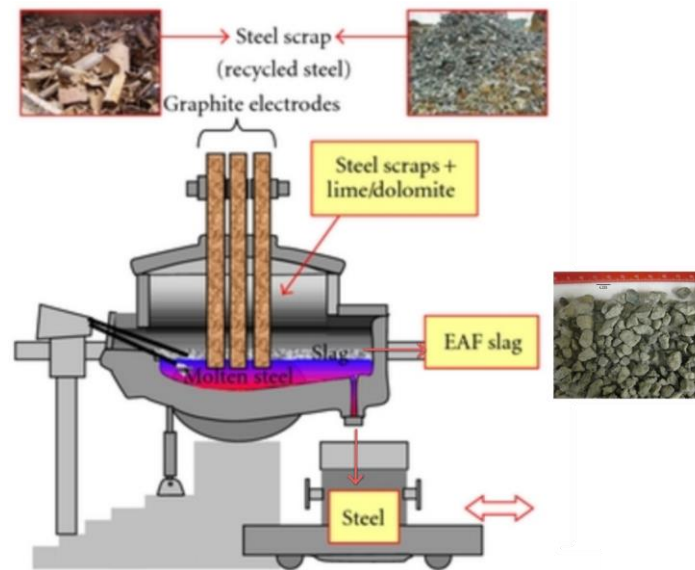


A final crystallization and drying process using $\text{NaNO}_3 + \text{KNO}_3$ then results in a favorable mix of the solar salt with high purity (99.6 %) which is required for the application in TES systems.

2.3.2 EAF slag filler material

The electric arc furnace is the process for steel production from steel scrap materials. During this steel making process in the electric arc furnace, some of the undesirable materials (e.g. manganese, silicon, lime, etc.) oxidize during the melting process (at approximately $1'480^\circ\text{C}$) and enter the slag phase. The slag forms a separate layer on top of the steel liquid and is eventually separated (Figure 12).

Figure 12: Flow diagram of the electric-arc-furnace steelmaking process.



From there, the slags are poured into pot carriers and eventually brought to a slag pit where the slag is air-cooled and stockpiled. If the cooling process is accelerated via water spraying, it leads to cracking which simplifies further processing, similar to digging and crushing in the case of the slags utilization. However, the cooling process is also essential since it drastically affects the physical and mineralogical properties of the material. The chemical composition of the EAF slag depends significantly on the properties of the recycled steel introduced into the furnace. Chemical characterizations of the Slagstock's project partner, Arcelor Mittal Sestao, EAF slag reveal mainly iron oxides (37 wt%), lime (26 wt%), and silica oxides (14 wt%), which are refractory and fluxing oxides making them quite close to ceramic or refractory materials.

The EAF slag is a by-product of the steelmaking industry, the recovery of which reduces landfill waste and helps to preserve natural resources. Of the total EAF steel produced, about 15 to 20% slag is collected (Zhang, Liu, Liu, & Yang, 2011) and, of that amount, 85% is re-used, either in road construction, as construction aggregates for the surface layers of pavement and asphaltic layers, or in the cement and concrete production. The remaining EAF slag is considered an industrial waste product (EUROSLAG – The European Slag Association, 2017). Arcelor Mittal (AM) Sestao generates about 150 kg of slag per ton of liquid steel which, on average, amounts to approximately 130'000 tonnes per year in this single plant.

In WP1 of the Slagstock project, thermo-physical and structural characterization of this raw EAF slag (e.g. thermogravimetric analysis, thermal expansion, thermal conductivity, compression strength, bend test, and compatibility with molten salt and

air at 800°C) were performed with the result that it is a fully feasible and highly suitable filler material when using molten solar salt and air as HTF within the envisioned operation temperatures (Ortega-Fernandez, et al., 2015). Given this favorable characterization of the EAF slag, the use of it as a sensible heat storage material leads to a potential cost-effective, high temperature storage solution for both current and future TES technologies incorporated in CSP plants.

The EAF slag raw material is not, however, suitable to be used directly as a filler material in a storage tank, since the geometrical shapes are not unified. Numerical modelling and parametric analysis (Slagstock's WP 2) revealed that larger particle diameters in the packed bed of a thermocline tank leads to lower storage capacity, however, pressure drops increase drastically with particle diameters smaller than 10 mm and larger tank aspect ratios¹⁸.

A large pressure drop in the thermocline tank is particularly difficult to handle in the packed bed system using air as a HTF because of the increased pumping energy requirements. In the case of the HTF molten solar salt, pumping losses are negligible. To minimize the tank size, low tank aspect ratios and particle diameters are favorable as they also lead to higher thermal storage capacities and significant pressure drop reductions induced by the packed bed. Results of the numerical models revealed that EAF slag pebbles with a diameter of 10 mm are preferable and recommend tank aspect ratios of 2 for the molten solar salt system and 0.25 for the air-based system.

Several methods to manufacture EAF slag pebbles with spherical shapes and diameters of 10 – 20 mm were investigated:

- Sintering method
- Pouring method
- Mechanically conformation

The sintering procedure developed by the Slagstock project partner, Tellus Ceram, involves a cold rolling method (25 – 50°C) which uses a high content of pure EAF slag (82 – 85%) and approximately 20% of binder materials. After sorting the slag raw materials and further crushing and grinding them down, the developed recipe is

¹⁸ The aspect ratio represents the height to diameter relationship of the storage tank. It is chosen based on the TES system behavior and requirements.

established and mixed. The desired spheres are formed during the cold shaping process by implementing this cold rolling method and are left to dry when they pass quality control. During the cooking process, the pebbles are placed in a chamber within the cooking train and then transferred into the sintering oven where they are cooked at temperatures above 1200°C for approximately two days (Figure 13).

Figure 13: EAF slag pebbles produced via the sintering method developed at Tellus Ceram.



Using this method, a large amount of slag pebbles can be produced with favorable characteristics and the sintered slag pebbles will be tested in the Slagstock pilot plant (WP4).

Two types of melting and pouring methods were tested by Slagstock project partner, IK4-Azterlan, but were eventually discarded and not further pursued. The pouring process became difficult for small diameter pebbles production using their casting or pouring methodology with 70 mm being the lowest production diameter they could achieve (Figure 14).

Figure 14: Indirect slag melting through a graphite crucible (1500°C) and pebbles pouring into sand moulds during the casting process.



Additionally, the production of large amounts of pebbles presented significant limitations due to the high viscosity of the slag melt, ultimately leading to the conclusion that this method is not technically or economically feasible.

An alternative production pathway studied is the mechanical conformation of the raw material itself (Figure 15). The raw material is crushed into smaller particles (12 – 25

mm) and further processed in a tumbler for approximately 25 hours. During the tumbling process, a noticeable amount of dust occurs requiring the slag pebbles to be cleaned with water and dried with air after the deformation.

Figure 15: Crushed EAF slag particles (left). An industrial concrete mixer was used to mechanical conform the EAF slag raw material in order to obtain quasi-spherical geometry (right).



While this method will allow for large scale production, only a limited sphericity of the EAF slag pebbles within the acceptable tolerance can be established with an overall efficiency of around 60% and a discarding rate of 40%. Nevertheless, the mechanical conformed method represents a feasible alternative to produce slag pebbles in a cost effective way and the produced pebbles will be tested in the pilot plant.

For this LCA, the sintering method and the mechanical conformation method of the EAF slag pebble production are considered.

3 LIFE CYCLE ASSESSMENT METHODOLOGY

An LCA is an important tool to better understand the environmental performance of systems and products. The aim is to quantify the environmental footprint of goods by taking into account the complete life cycle, starting from the production of raw materials and ending with the final disposal of the products, including material recycling if needed.

The LCA method falls within the environmental management standards of the International Organization for Standardization (ISO) and includes ISO 14040 and ISO 14044 specifications. In compliance with ISO 14040 (2006) and 14044 (2006), the LCA is carried out in four distinct phases:

- Goal and scope definition
- Life cycle inventory (LCI)
- Life cycle impact assessment (LCIA)
- Interpretation

The fundamental analysis of LCA studies consists of establishing mass and energy balances of the studied system from cradle-to-grave. In this way, the inputs and outputs are identified with potential environmental impacts later evaluated.

A cradle-to-grave approach involves analyzing all the steps in the product production, from raw material extraction and transport, to production and consumption, and eventually re-use or the disposal. Applying this method, the life cycle of a product, service, or system can be modeled.

3.1 Goal and scope definition

In order to ensure a LCA consistency, the definition of a goal and scope is a critical part of an LCA due to their strong influence on the result of the LCA. The goal definition has to define the intended purpose of the study and users of the results.

The scope of the LCA establishes the boundaries of the assessment in order to clarify the expected depth of the study and the compatibility and sufficiency required to address the stated goal. In order to define the scope, the system or product in focus needs to be described because the understanding of it is important also in the data collection phase and in finding alternatives to be included in the study.

The definition of functional units, or performance characteristics, is the foundation of an LCA because the functional unit sets the scale for the comparison of two or more products, including improvements to one product (system). It provides a reference to which the input and output flows of the system are normalized. To determine the

system boundaries, the geographical boundaries, life cycle (i.e. limitations in the life cycle) boundaries, and boundaries between the technosphere and biosphere should be considered.

Ideally, the product system should be modelled in such a manner that the inputs and outputs at its boundaries are elementary flows. However, the lack of time, data, or resources to conduct such a comprehensive study typically limits the level of detail of the evaluation and minor or negligible inputs and outputs that will not significantly change the overall conclusions of the study should be determined and subsequently omitted.

3.2 Life cycle inventory

The LCI phase determines all relevant input and output flows of the system to-and-from nature and the technosphere¹⁹. It includes data collection, refinement of system boundaries, calculations, validation of data, relation of data to specific systems, and allocation. The data can be site specific (e.g. from specific companies, specific areas, and from specific countries), but also more general (e.g. data from more general sources: trade organizations, public surveys, etc.). Therefore, the data can be quantitative or qualitative and should be collected for each unit process that is included within the system boundaries.

Procedures used for data collection vary depending on the scope, but in many cases average data from the literature (often previous investigations of the same or similar products or materials) or data from trade organizations are used, providing a conceptual or simplified evaluation. However, collection of specific system data is required for a more detailed LCA which involves a literature survey and the preparation of questionnaires in order to discuss and obtain the required data from specific manufacturers, logistic companies, etc.

There are no formal demands for calculations, but due to the amount of data, it is recommended as a minimum to develop a spreadsheet for the specific purpose.

3.3 Impact assessment

The purpose of a Life Cycle Impact Assessment (LCIA) is to assess a system's LCI results with the aim of improving the understanding and evaluating the potential environmental significance of a system or product. LCIA specifically uses impact categories and associated indicators to simplify LCI results with regard to one or

¹⁹ The technosphere is more simply defined as the man-made world.

more environmental issues. An LCA shall include LCIA to help identify potential environmental problems associated with various man-made activities.

An important step in the LCIA is the selection of the appropriate impact categories which is guided by the goal of the study. To date, consensus has not been reached on one single default list of impact categories. However, Bauer et al. (2017) points out: “Potential impacts on climate change – measured in terms of life-cycle GHG emissions – are in the center of national and international energy and environmental policy and at the same time represent the most important burden of the current global electricity supply.”

Therefore, life-cycle GHG emissions and their associated impacts on climate change are used as main indicators for the environmental performance of the systems in this study. Further indicators are provided and are discussed in less detail. The selection of indicators is based on the recommendations by the International Reference Life Cycle Data System (ILCD) (EC, 2010), (Hauschild, et al., 2013) and are assessed by the ILCD 2011 Midpoint+ v1.09 LCIA method.

The potential global warming or greenhouse effect is normally quantified by using *global warming potentials* (GWP) for substances having the same effect as CO₂ in reflection of heat radiation. GWP for greenhouse gases are expressed as CO₂-equivalents, i.e. their effects are expressed relatively to the effect of CO₂. Global warming potentials are developed by the “Intergovernmental Panel on Climatic Change” (IPCC) for a number of substances (IPCC, 2013). GWPs are normally based on modelling and are quantified for time horizons of 20, 100 or 500 years for a number of known greenhouse gases (e.g. CO₂, CH₄, N₂O, CFCs, HCFCs, HFCs and several halogenated hydrocarbons, etc.). All GHG emissions assessed in this study were established by the IPCC 2013 GWP 100a LCIA method. The potential greenhouse effect of a process can be estimated by calculating the product of the amount of emitted greenhouse gas per kg produced by a material and the potential for greenhouse effect given in kg CO₂- equivalents per kg for each gas. Finally, the contribution to the potential greenhouse effect from each gas has to be summarized.

3.4 Interpretation

Interpretation is the fourth phase in an LCA containing the identification of significant environmental issues, evaluation, conclusion, and recommendations. The interpretation takes place continuously throughout the course of the LCA, improving it by, for example, revising the system boundaries, further data collection, etc. This

iterative process must be repeated until the requirements of the goal and scoping phase are fulfilled.

The aim of the interpretation phase is to identify the key results needed to facilitate a decision making process based on the LCA study.

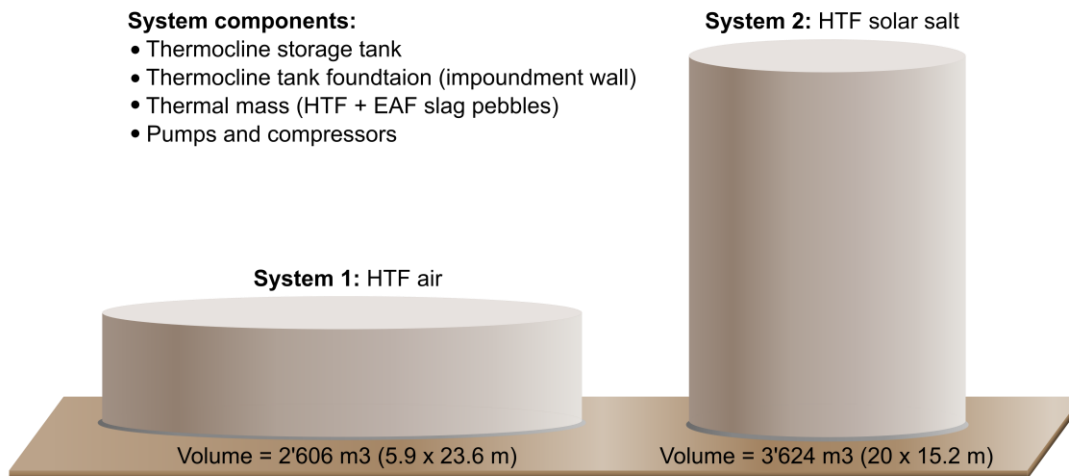
The following chapters describe the four previous mentioned phases of an LCA. Chapter 4 represents the goal and scope phase, chapter 5 describes the life cycle inventory, chapter 6 presents the results of the LCIA, and chapter 7 provides the interpretation of the results, where conclusion are respectively discussed.

4 DESCRIPTION OF EAF SLAG-BASED STORAGE SYSTEMS STUDIED

The goal of this LCA is to evaluate the environmental impact of the innovative Slagstock packed bed TES system which is composed of a thermocline tank filled with EAF slag pebbles as a sensible heat storage material, and is operated with air (system 1) or molten solar salt (system 2) as HTF for CSP tower applications, as illustrated in Figure 16.

TES systems are generally comprised of several components. In the process of investigating their environmental burden, segmentation of the system helps to better identify what and how much affects which element, thus enhancing interpretational conditions. The required components can be identified as: the storage vessel, the tank foundation, the tank content or thermal mass, and the pumps and compressors.

Figure 16: Thermocline TES system designs: EAF slag-based with HTF air (system 1) on the left and with HTF molten solar salt (system 2) on the right. The illustration ratio between both packed bed systems is 1:1.



Both EAF slag-based packed bed systems are designed to generate electricity via a conventional steam Rankine cycle compatible with a 50 MWe steam turbine generator. One of the defined heat storage requirements for this 50 MWe CSP plant is a 6 hours storage capacity, leading to a thermal capacity of 1 GWht. Each thermocline design (e.g. tank dimensions, thermal mass, and its flow rate, etc.) depends on the plants HTF specification and has to be modified to meet its specific heat capacity and operating temperature range. For this reason, both systems vary from one another.

Table 3: Design configurations of the thermocline TES system for the application for HTF as air (system 1) and molten solar salt (system 2).

Design settings	System 1	System 2	Unit
Steam turbine capacity		50	MWe
TES thermal capacity		1	GWht
TES storage capacity		6	h
HTF temperature range	RT ^a – 800	290 – 565	°C
EAF slag mass	5'992	8'334	t
EAF slag particle diameter		10 – 20	mm
Fluid mass	0.57	2'441	t
Void fraction		0.37	
Thermocline tank volume	2'602	3'624	m ³
Thermocline tank diameter	23.6	15.2	m
Thermocline tank height	5.9	20	m
Fluid flow rate	201	310	kg/s
Pressure drop	7'130	870	Pa
Turbine efficiency	0.3	0.4	

^a Room temperature

The design parameters of the two packed bed systems (Table 3) were established and modelled in WP 1 and 2 of the Slagstock project. The thermocline tanks have a cylindrical shape and are designed to allow for thermal expansion of the HTF and filler material, and the void fraction in the packed bed of the thermocline vessel is configured to reach suitable heat storage – pressure drop conditions. Based on these design configurations, the LCI was compiled.

For each of the two systems, the two selected EAF slag pebble production methods proposed and manufactured within WP 3 of the Slagstock project, namely (a) the sintering production method and (b) the mechanical conformation method are investigated. This results in four approaches that are evaluated and compared.

- System 1a: direct air packed bed system including sintered EAF slag pebbles.
- System 1b: direct air packed bed system including mechanical conformed EAF slag pebbles.
- System 2a: direct molten solar salt packed bed system including sintered EAF slag pebbles.
- System 2b: direct molten solar salt packed bed system including mechanical conformed EAF slag pebbles.

The environmental performance is quantified and discussed with a focus on life-cycle greenhouse gas (GHG) emissions. Other selected performance indicators are provided based on the recommendations by Hauschild, et al., (2013).

Additionally, the slag-based TES systems can be put into perspective by examining other alternatives. One particular LCA of interest compares the embodied life-cycle GHG material emissions of molten solar salt indirect two-tank and indirect thermocline TES systems, both of which are designed to supply 6 hours of thermal storage for 50 MWe CSP plants, and, therefore, offer suitable comparability conditions (Heath, et al., 2009) published by the National Renewable Energy Laboratory, NREL. For this reason, the following LCA evaluates the embodied GHG emissions of the EAF slag-based TES system at first for the purpose of maintaining comparability.

Telsnig (2015) in his LCA of location-specific solar thermal power plants in South Africa evaluates the environmental impact of CSP plants using two-tank molten solar salt indirect and direct TES systems. The dataset of Telsnig's LCA was shared with the author and provides an important set of detailed material inventories on commercially operated CSP and TES technologies. Telsnig (2015) introduces a scaling method in his LCA that allows for the resizing of an engineered CSP reference plant. The LCAs of both, Heath et al. (2009), and Telsnig (2015), are based on a CSP conceptual reference design from Kelly (2005), (2010), and, therefore, provide a reliable basis to compare the various technologies.

It is worth noting that Kelly's reference plants, one being a 250 MWe CSP parabolic trough plant with 3 hours of thermal storage (two-tank, indirect, molten solar salt design), and the other being a 440 MWe CSP central receiver design with a 11'460 MWht two-tank, direct, molten solar salt heat storage, were never built nor operated. Nevertheless, the 250 MWe parabolic trough design followed the design of the 50 MWe AndaSol1 CSP parabolic trough project in Spain which includes a 7.5 hour, two-tank, indirect, molten solar salt thermal storage option (Solar Millenium, 2008). The AndaSol1 plant has been generating electricity since 2008. The 440 MWe CSP central receiver reference design is based on the Solar Two project (10 MWe CSP plant with a 110 MWht two-tank, direct, molten solar salt TES system), where the capability of the molten direct solar salt TES technology was researched (Pacheco J. E., 2002). Eventually the Solar Two plant was demolished after many years of successful demonstration in 2009.

By combining the above mentioned LCA studies on large-scale operated TES systems from NREL (Heath, et al., 2009), and Telsnig (2015) with the Slagstock's evaluated EAF slag TES technology options, a comparison can be made of the embodied life-cycle GHG emissions of five individual TES systems for a 50 MWe CSP plants as illustrated in Figure 17.

Figure 17: Overview of the LCA TES system comparison.

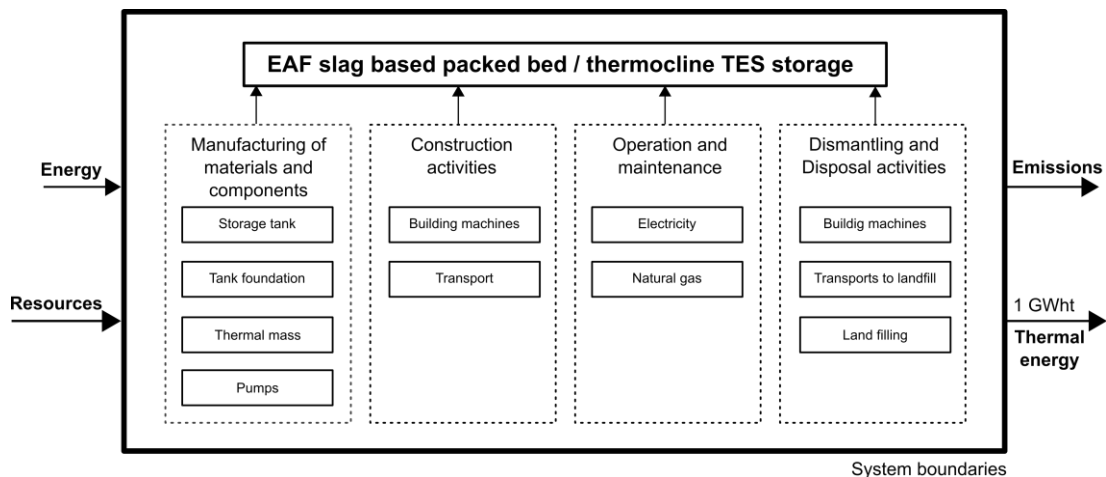
	(Slagstock)		(Telsnig)	(NREL)	(Telsnig)
TES system	1	2	3	4	5
HTF	AIR		MOLTEN SALT		
	RT - 800°C	290 - 565°C		290 - 390°C	
Storage material	EAF slag pebbles		molten salt	quartzite rock & sand	molten salt
EAF slag pathway	(a) Sintering	(b) Mechanical conform.			
Design	THERMOCLINE		TWO-TANK	THERMOCLINE	TWO-TANK
CSP Application	TOWER (direct)			TROUGH (indirect)	

This comparison provides an initial assessment of the various TES technologies which are described in detail in chapter 2.2.1, and gives an overview of the individual environmental burdens.

The lifetime of the investigated EAF slag-based TES system is expected to reach 30 years and the assumption is made that the operational conditions require a fully charge and discharge procedure.

In order to establish the days of operation throughout its life-cycle, the DNI weather records of the final TES location provide valuable baseline data. Using these assumptions, the functional unit of the EAF slag-based packed bed solution is chosen to represent a 6 hours and 1 GWht of thermal storage capacity for 50 MWe CSP tower plants. Figure 18 shows the system boundaries of the considered EAF slag-based TES system.

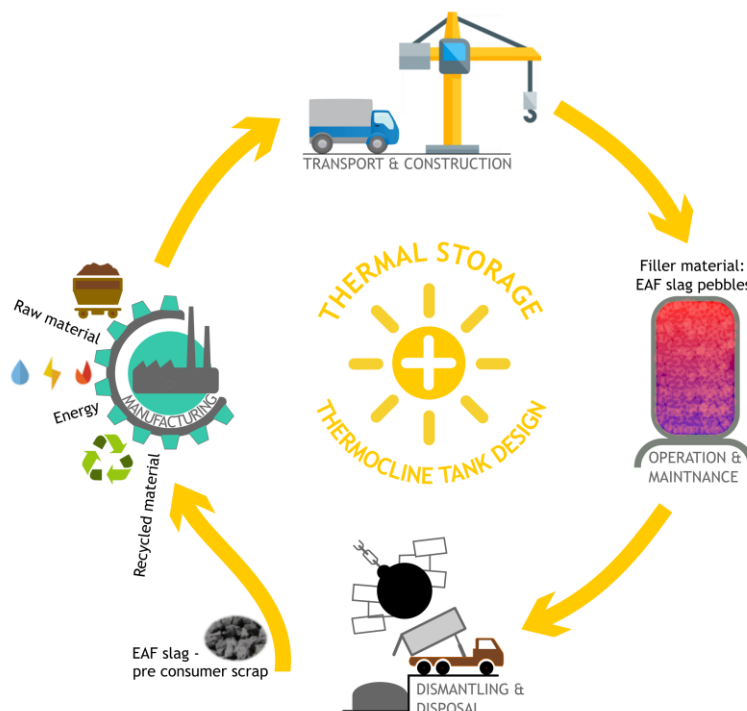
Figure 18: System boundaries of the life cycle of the EAF slag-based thermocline TES storage solution. The energy and resources requirements for all necessary components and life-cycle stages are considered in order to establish the environmental impact of the investigated TES system. The functional unit represents a 1 GWht thermal storage capacity for a 50 MWe CSP central receiver plant located in Seville, Spain.



The LCA considers all stages of the EAF slag-based TES system from cradle-to-grave factoring in the manufacturing of materials and components, construction activities, operation and maintenance, and dismantling and disposal activities. The location of the EAF slag-based packed bed storage solution is chosen to be in Seville, Spain, since the Slagstock project is a European network R&D initiative and a number of commercial CSP plants have already been realized in southern Spain. Figure 19 shows a more illustrative visualization for the life cycle of the packed bed heat storage, pointing out that the EAF slag is considered to be *pre-consumer scrap*. This means that the EAF slag is utilized, and, therefore, prevented from being landfilled. For this reason, this LCA considers the EAF slag raw material to be environmentally neutral or “burden-free”.

As for the disposal of all steel masses used in this LCA, a recycling rate of 54%, which is the steel recycling ratio in the EU-28 from 2013 – 2016 (Bureau of International Recycling, 2017), is expected and account for.

Figure 19: Simplified illustration of the complete life cycle for the EAF slag-based packed bed heat storage. It includes resource extraction and manufacturing, transport and construction, operation and maintenance, and dismantling and disposal. The EAF slag is considered to be a pre-consumer scrap.

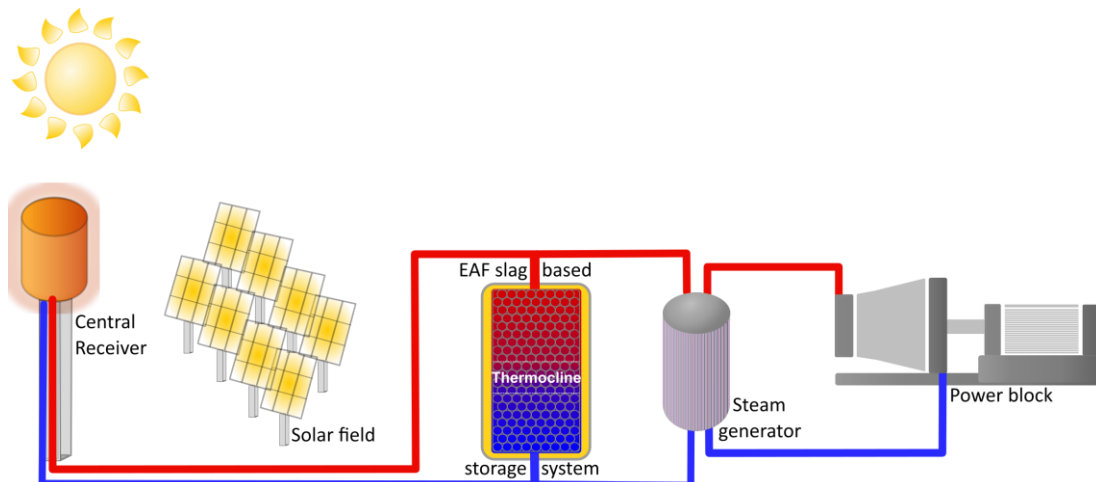


As discussed earlier, the TES system is only one component of the complete CSP plant. In addition to the comparative TES-study, if one wants to allocate the EAF slag-based packed bed GHG emissions per unit of STE generated electricity (kWhe), it is necessary to include all components of the complete CSP plant in the

LCA. Since the slag-based TES system is designed to be implemented within a CSP tower plant due to its higher HTF temperature requirements (565 and 800°C), the LCA of the complete CSP system will only factor in the implementation of the investigated direct TES system within CSP central receiver applications. However, LCA results are currently only available for commercial CSP central receiver plants with HTF molten solar salt in operation (system 2). Unfortunately, very few engineering details on the less mature CSP volumetric air receivers can be found in the literature and, considering the timeframe of this Master's Thesis, it was therefore only possible to evaluate the LCA of a complete molten solar salt CSP tower plant which incorporates the EAF slag-based TES system 2.

A CSP central receiver plant with the EAF slag-based, packed bed storage system can be segmented into three separate sections: a solar field, a thermal storage, and a power block (Figure 20). The solar field includes the collector field, where heliostats tracking the sun's path throughout the day, and the solar tower receiver where solar energy is absorbed by the HTF. The thermocline tank, which consists of a storage tank, tank foundation, thermal mass, and pumps, is in direct contact with the HTF, and, therefore, requires no additional heat exchanger. The power block runs a Rankine steam cycle where sufficient steam is produced via a heat exchanger (steam generation system) to drive a 50 MWe steam turbine and its generator. A down-stream condenser allows for the recycling of the freshwater.

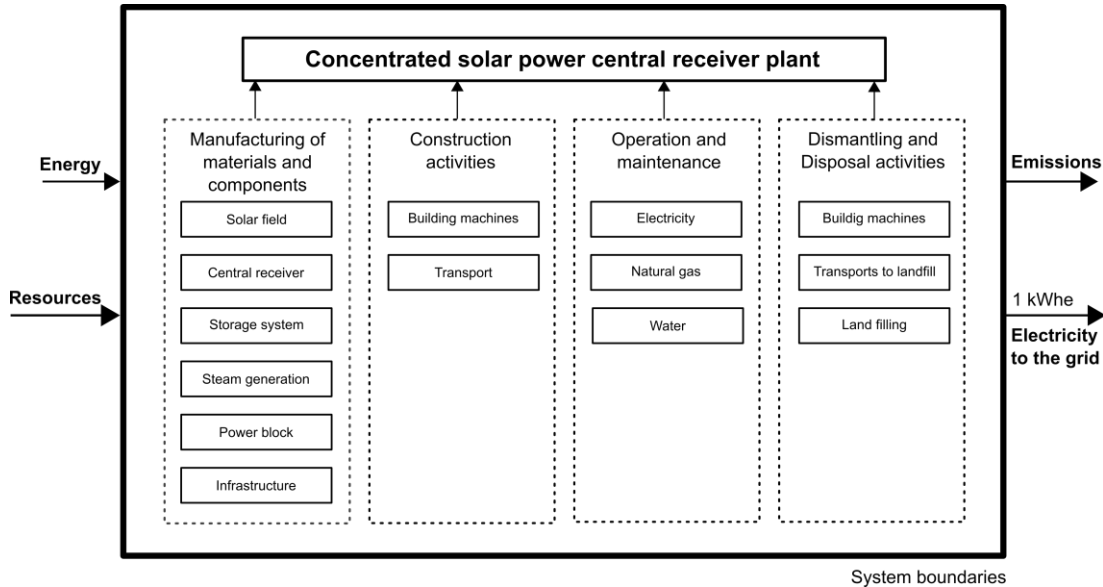
Figure 20: Simplified illustration of a CSP central receiver plant layout consisting of a solar field, thermocline TES system, steam generator, and power block. The solar energy absorbed by the receiver is used to drive a steam cycle for electricity generation. Depending upon the actual heat demand, excess thermal energy charges a large insulated storage tank, allowing for stable and dispatchable power generation also at times without sunshine.



The system boundaries of the complete 50 MWe CSP central receiver plant (Figure 21) include all life cycle stages of the required system components. The CSP plant

installation location is Seville, Spain, and is chosen to operate as a solar only STE generation system. This means that the CSP plant does not feature a co-firing system.

Figure 21: System boundaries of the life-cycle of a CSP central receiver plant. The energy and resources requirements for all necessary components and life cycle stages are considered in order to establish the environmental impact of the CSP plant. The functional unit represents a 1 kWhe electricity output for a 50 MWe CSP central receiver plant including 6 hours of EAF slag-based thermal storage located in Seville, Spain.



With respect to the LCA data collection for the 50 MWe CSP central receiver plant using molten solar salt as an HTF, the shared material inventories of Telsnig (2015) provide quantitative and solid fundamental information and was therefore adapted for this LCA.

The material inventories for a 20 MWe CSP tower plant segmented into its components was provided in a spreadsheet and allowed the application of a scaling method which was also introduced by Telsnig (2015) in order to scale down a 440 MWe CSP tower reference system. For the adaptation of the scaling method the following parameters need to be established:

- Solar field size (m²)
- Thermal storage capacity (MWht)
- Plant electricity capacity (MWe)
- Steam mass flow rate (kg/s)

5 INVENTORY COLLECTION

5.1 Thermocline storage tank

The design parameters for the Slagstock proposed EAF slag packed bed thermocline tank system 1 (air design) and system 2 (molten solar salt design) have been assessed by the modelling efforts within WP 2 of the Slagstock project and their material inventories are based on the resulting design configurations as shown in Table 3. Based on this, the author developed a suitable TES design following engineering specifications from the literature, which was discussed and agreed upon with the Project partners. The inventory mass was calculated using the material dimensions and an average density (Table 4). The manufacturing pathways a, and b (sintering process, and mechanical conformation) of the filler material EAF slag pebbles does not depend on the tank design. However, the HTF used and its operation temperature range influence the tank design.

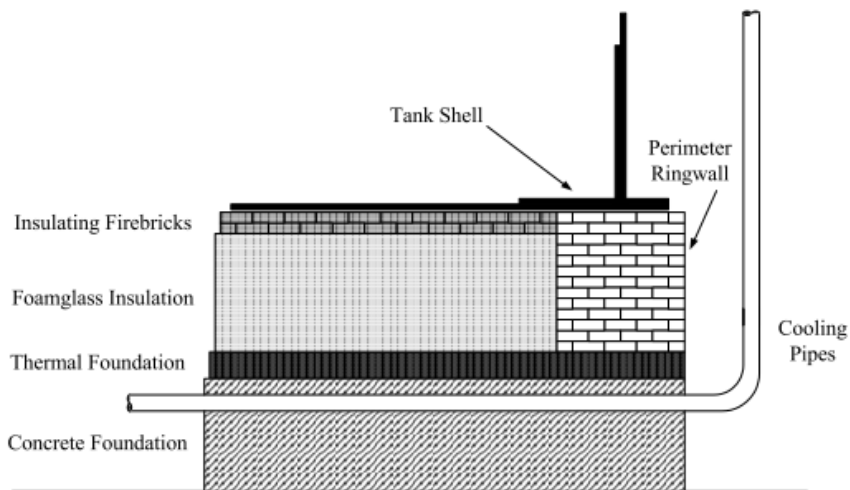
With regard to the material selection of the tank vessel itself, the temperature and pressure requirements of the process led to a decision that the tank shell should consist of stainless steel. Stainless steel was proven to be compatible with EAF slag at high temperatures and is commonly used as the hot tank material in two-tank TES system configurations.

Table 4: Assumed densities of used bulk materials.

Density	kg/m ³
Carbon steel	7'850
Stainless steel	7'640
Calcium silicate	295
Mineral wool	160
Foam glass	110
Firebrick	623
Concrete	2'380
Concrete rebar (per m3 of concrete)	7.3

Starting from the bottom of the EAF slag-based thermocline system configuration, the tank foundation consists of an insulated concrete foundation, a concrete slab, foam glass insulation, insulating fire bricks, and a steel slip plate, as illustrated in Figure 22. No active convection cooling is required in the assumed civil foundation design. The perimeter of the foundation is slightly adjusted between the two TES systems to support the large loads from the walls and the roof which consisting of a ring wall of fire bricks.

Figure 22: Thermocline tank foundation design (Kelly & Kearney, 2006)



Variations in the design parameters (Table 5) when comparing the thermocline tanks of system 1 and system 2 result mainly from the larger operating temperature range of the HTF's (765°C vs. 275°C) and, subsequently, changes in the thickness of the insulation material. The insulation material must be able to minimize heat losses to the surroundings and improve the efficiency and thermal ratcheting. Mineral wool and calcium silicate were selected as insulation materials.

Table 5: Thermocline storage tank insulation and foundation – Design specifications

Design specifications	System 1	System 2	Unit
Vessel thickness (stainless steel)	0.025	0.025	m
Floor thickness	0.0078	0.0078	m
Roof thickness	0.0066	0.0066	m
Insulation on wall - thickness average (calcium silicate)	0.5	0.375	m
Insulation for roof - thickness (calcium silicate)	0.5	0.375	m
Insulation material - thickness (mineral wool)	0.58	0.23	m
Firebrick on foam glass	0.0572	0.0572	m
Foam glass insulation on foundation	0.371	0.371	m
Firebricks on perimeter	0.428	0.428	m
Steel slip plate (carbon steel)	0.00635	0.00635	m
Thermal slab (concrete)	0.0792	0.0792	m
Concrete foundation	0.61	0.61	m
Impoundment wall height (concrete)	-	3.0	m

For system 2, the HTF molten solar salt requires that the thermocline vessel design provide ullage space at the top to accommodate approximately 10% thermal expansion of the molten solar salt volume during operation. Since the thermocline tank is filled with EAF slag pebbles, two gravity-fed surge tanks with short shafted pumps are used at the hot and cold ends of the thermocline tank. This design

simplifies pump maintenance and will allow for easier access, as suggested in Libby (2010).

During the initial process of filling solar salt into the storage tank of system 2, an electric continuous flow heater provides the heat source to melt the solar salt to temperatures above 220°C in a sump tank made of carbon steel. A hot-gas generator combined with a rotary blower then preheats the storage tank and the filler material to prevent damage to the tank from thermal stress and ensures that the solar salt does not freeze on any cold spots during the initial fill. During stand-by operation of the system 2 (between charging and discharging), a small amount of molten solar salt is always required to circulate throughout the system to maintain the temperature above the freezing point. In the event that the temperature of the molten solar salt drops below the freezing point, all lines will be drained and an auxiliary tracing system will protect the molten solar salt from freezing if required.

Furthermore, the use of molten solar salt requires the construction of an impoundment wall, which is a safety measure that follows the guidelines provided by NFPA 59A (Libby, 2010) to ensure molten salt containment in the event of a tank failure. However, the installation of an impoundment wall is not necessary in case of system 1, since air is not a polluting substance.

The installation of instruments and sensors are not taken into account as the impact was found to be rather marginal. For the pump inventory, a material listing and the defined scaling factors (Telsnig, 2015) provide the estimates of the material components and their masses needed for the thermocline tank design.

The complete thermocline storage system design requirements for both, system 1 and system 2, are presented in Appendix D.

The raw material and energy requirements for the production of solar salt and the manufacture of the EAF slag pebbles are described in the following sections.

5.2 Mined solar salt

The material and energy requirements were collected in direct collaboration with the leading producer, SQM (Casubolo, 2017). A questionnaire was created in order to allow for easy data exchange. Through further correspondence, more detailed questions also provided reliable background data. The LCI for the production of mined solar salt is established via four processes: caliche ore extraction, production of sodium nitrate, production of potassium chloride, and the production of the solar salt. The inventory lists are reported in Appendix G. The processes are based on the description in section 2.3.1.

5.3 EAF slag filler material

In the manufacturing of the EAF slag pebbles, two methods were considered (as described in Chapter 2.3.2): the sintering process and the mechanical conformation of the raw material.

Table 6 lists the raw materials required for the production of 1 kg sintered EAF slag pebbles. The material inventory list is based on the special recipe and cooking process developed by the Slagstock project partner, Tellus Ceram, and was established via direct communication with the manufacturer.

Table 6: Material inventory for the production of 1kg sintered EAF slag pebbles using several production steps: crushing, rolling, mixing, drying, and cooking.

INPUT for the production of 1kg sintered EAF slag pebbles	Quantity	Units	SINTERING PLANT Raw material - Crushing - Rolling - Mixing - Drying - Cooking Quality control Transport	OUTPUT for the production of 1kg sintered EAF slag pebbles	Quantity	Units
EAF slag	1	kg			EAF slag pebbles	1
Clay	0.21	kg				
Tap water	0.088	kg				
Sodium silicate	0.0017	kg				
Surfactant (Ethylene oxide)	9.00E-07	kg				
Electricity	0.5	kWh				
Natural Gas	7.2264	MJ				
Transport	900	kgkm		Inert material landfill	0.1	kg

Energy requirements for the cooking process were calculated using the actual amount of natural gas consumption by the sintering furnace at the plant, the cooking duration of the EAF slag pebbles, and the production rate. After quality control of the finished product was performed, approximately 10% was considered to be unsuitable and was disposed of as an inert material in landfills. Transportation of the EAF slag pebbles from the location of the steel industry (Bilbao, Spain) to the location of the CSP plant (Seville, Spain) was taken into account.

Table 7 provides the inventory listing of the EAF slag pebble production via the mechanical conformation method. The material inventory list was developed via direct communication with the corresponding contact at AK4-Azterlan, the Slagstock project partner that produced the pebbles for testing in the constructed pilot plant. There were no additional raw material requirements for this process. Due to the formation of slag dust, water was used in the cleaning of the pebbles after the tumbling process.

Table 7: Material inventory for the production of 1kg mechanical conformed EAF slag pebbles via tumbling, washing, and air drying.

INPUT for the production of 1kg mechan. conform. EAF slag pebbles			MECHANICAL CONFORMFORMATION Raw material - Tumbling - Washing - Drying Quality control Transport	OUTPUT for the production of 1kg mechan. conform. EAF slag pebbles		
	Quantity	Units			Quantity	Units
EAF slag	1.64	kg		EAF slag pebbles	1	kg
Water	1.69	kg		Particles to air (unspecified)	0.04	kg
Diesel burned in machines	2.36	MJ		Inert material landfill	0.6	kg
Transport	900	kgkm		Wastewater avg.	1.69	l

The energy requirements of the tumbling process were calculated based on the amount of diesel consumption by an industrial concrete mixer vehicle, the tumbling duration, and the production rate. After the cleaning process, the EAF slag pebbles were air dried.

The rejection rate of 60% after the quality control is much higher in comparison to the sintering method. The dust rate was assumed to be 4%. The transportation of the EAF slag pebbles to the TES construction site is considered to be the same as for the sintering process (Bilabo to Seville).

5.4 Alternative TES system comparison

In order to allow for an adequate comparison of the proposed EAF slag packed bed thermocline storage systems 1 and 2 with LCAs of common two-tank TES systems, as well as an alternative theoretical quartzite, sand packed bed, thermocline system, the embodied GHG emissions results of all TES systems (Figure 17) were modelled using the SimaPro Software v8.3 in combination with Ecoinvent v3.3 life cycle inventory database.

Material inventories from Telsnig (2015) and Heath, et al., (2009) were used, adjusted, and scaled accordingly. The material inventories of these comparative TES system designs (systems 3 – 5) are listed in Appendix D.

This comparison evaluated embodied life-cycle GHG emissions from the materials and energy required to supply 6 hours of thermal storage for 50 MWe CSP plants. Construction and decommissioning related GHG emissions were not taken into account here, as it was not expected to significantly affect the relative results. For the TES systems operating with the HTF molten solar salt (system 2 – 5), auxiliary electricity consumption from night-time circulation of the HTF and heat tracing efforts were estimated to require 11'990 kWh for two-tank configurations (Whitaker, et al., 2013) and approx. 4'000 kWh for thermocline systems.

When TES systems reach the end of life, the steel inventory can be profitably recycled and reused for future plants as no hazardous materials are used in the

system (Teske, 2016). For this reason, a steel recycling rate of 54% from the EU-28 (Bureau of International Recycling, 2017) is factored in to account for the disposal of the steel material mass.

5.5 50 MWe molten solar salt CSP central receiver plant including EAF slag-based TES system

A CSP plant is typically organized into the following components:

- Plant infrastructure
- Solar field
- Receiver system
- Thermal energy storage
- Steam generator system
- Power block

The System Advisor Model (SAM) was used to establish important CSP tower design parameters in order to account for material and energy requirements. SAM is a modeling software package (TRNSYS transient systems) developed by NREL. This model can simulate the electricity output of photovoltaic (PV), concentrating PV (CPV) and CSP plant including TES systems for many locations. For a CSP plant, SAM models the solar field, two-tank TES unit, and power block on an hourly basis to provide the annual performance (Dobos, Neises, & Wagner, 2014).

Based on weather data from Seville, Spain, (DNI 2073 kWh/m²/a) and a solar multiple of two, SAM models a 50 MWe CSP central receiver plant design with the solar field area of 449'872 m² (Table 8) and an average annual electricity output of 111.6 GWhe. The lifetime of the CSP tower plant is expected to reach 30 years.

Table 8: Results of the design parameter simulation by SAM modelled for a 50 MWe CSP tower plant located in Seville, Spain.

50 MWe CSP tower plant	Value	Unit
Receiver height	21	m
Receiver diameter	17	m
Receive thermal power	243	MWt
Tower height	193	m
Heliostat area	144	m ²
Heliostat count	6346	
Solar field area	449'872	m ²

In order to establish some steam generation system design parameters the steam turbine needs to be specified. Table 9 shows steam turbines specifically designed for CSP applications from Siemens and the SST-300 turbine seems to be suitable

for a 50 MWe CSP application which allows an inlet pressure of 120 bars (Siemens AG, 2010).

Table 9: Siemens CSP turbine specifications. The SST-300 steam turbine is suitable for a 50 MWe CSP plant and requires a steam inlet pressure of 12 MPa and a temperature of 520°C (Siemens AG, 2010).

Power output for Siemens steam turbines suitable for CSP

Type	Steam parameters	Output (MW)				
		50	100	150	200	250
SST-110	130 bar, 530° C					
SST-120	130 bar, 530° C					
SST-300	120 bar, 520° C					
SST-400	140 bar, 540° C					
SST-600	140 bar, 540° C					
SST-700	165 bar, 585° C	Dual casing / reheat or non-reheat				
SST-800	140 bar, 540° C	Single casing / reheat or non-reheat				
SST-800 & SST-500	140 bar, 540° C					
SST-900	165 bar, 585° C	Single casing / non-reheat		Dual casing / reheat		

The Steam System Modeler Tool (SSMT) from the U.S. Department of Energy is used to define the mass flow rate of the steam cycle. SSMT calculates all steam properties using the International Association for the Properties of Water and Steam's thermodynamic properties (IAPWS-IF97, 2007). Using the Siemens SST-300 required steam inlet pressure of 12 MPa and around 500°C in combination with a common steam outlet pressure of 20 kPa, SSMT calculated a steam inlet mass flow rate of 80 kg/s.

Using both system models (SAM and SSMT) to define the 50 MWe CSP tower plant design parameters, such as the solar field area and steam mass flow rate, leads to the ability to apply a scaling method. Scaling factors are a commonly used method to provide an estimation of the resource requirements from a reference system design and apply them to the investigated system size (Telsnig 2015). In this case, a material inventory list for a 440 MWe reference plant design from Abengoa Solar (Kelly B. , 2010) is used and scaled down to the 50 MWe CSP tower plant.

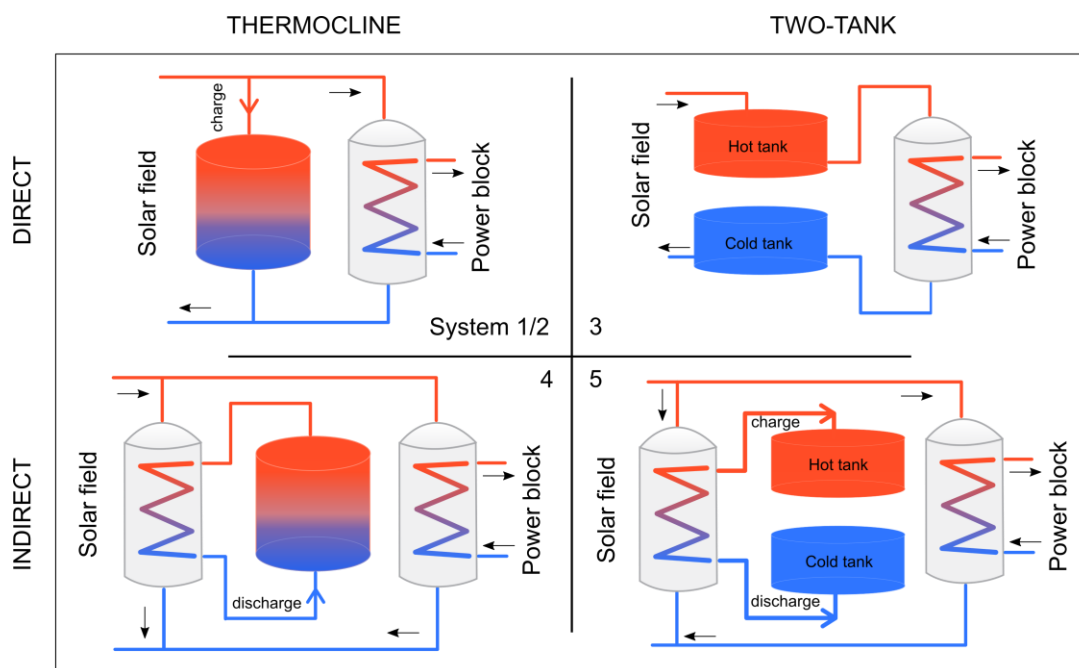
The material inventory for the 50 MWe CSP tower plant and the scaling factors are listed in Appendix E and F.

6 RESULTS

As described in chapter 4, a comparison of five individual TES technologies (Figure 17) is provided. The individual TES applications are illustrated in Figure 23 and are described in detail in chapter 2.2.1. Systems 2 – 5 are designed to operate with HTF molten solar salt and system 1 with air. Commonly used TES systems are based on molten solar salt indirect or direct CSP implementation in a two-tank configuration and the following results show the environmental burdens of mined solar salt in detail.

Systems 1 and 2 represent the Slagstock EAF slag-based thermocline systems. The EAF slag pebble filler material manufacturing: sintering process (pathway a) and mechanical conformation (pathway b) are also considered and presented.

Figure 23: Overview of the individual TES system application (system 1 – 5) evaluated in this LCA.



The software used for the realization of the LCA studies reported in this work is SimaPro (SimaPro v8.3, 2017) in combination with Ecoinvent v3.3 life cycle inventory database (Wernet, et al., 2016). The environmental burdens of the investigated storage materials, TES systems, and the CSP tower plant were assessed with a 100-year time horizon using the IPCC 2013 GWP factors to calculate the $\text{CO}_{2\text{eq}}$ emissions, the main indicator targeted in this work. Additionally, the ILCD 2011 Midpoint+ v1.09 method has been used to assess selected LCI indicators recommended by Hauschild et al. (2013). The Ecoinvent database v3.3 (allocation, cut-off by classification) is the source for the estimated GHG emissions

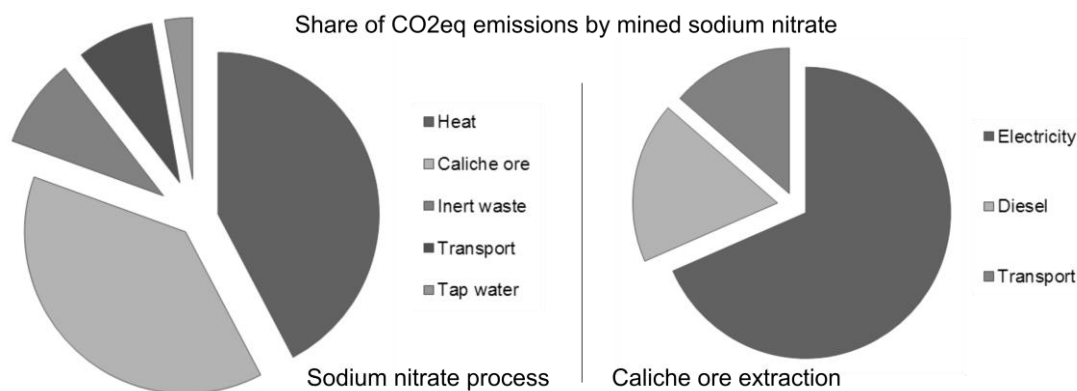
assigned to the individual materials analysed in this study (i.e., the background LCI database used).

The environmental impacts of the storage materials used are presented first, followed by the TES system comparison and finally, the results of the complete molten solar salt CSP tower plant are discussed. Finally, the CSP technology is put into perspective with alternative renewable and non-renewable electricity generation technologies to be used for Spanish electricity supply.

6.1 Mined solar salt

As detailed in chapter 2.3.1, solar salt consists of 60 wt% sodium nitrate and 40 wt% potassium nitrate. The manufacturing of mined solar salt is based on the production of sodium nitrate, potassium chloride, and its crystallization to potassium nitrate which eventually, after a finishing process results into the favorable mixture of the solar salt (Figure 10). Figure 24 shows the share of CO_{2eq} emissions by the production of sodium nitrate and, in more detail, the extraction of caliche ore (the source of sodium nitrate).

Figure 24: Share of CO_{2eq} emissions by mined sodium nitrate from SQM, Chile. The overall GHG emissions are estimated to generate 0.05 kgCO_{2eq}/kg.

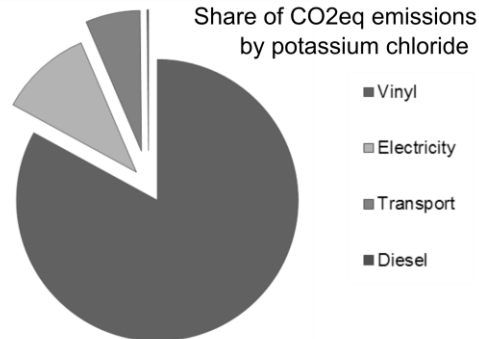


For the caliche ore extraction and crushing process GHG emissions of 0.012 kgCO_{2eq}/kg are estimated. Of this amount, 68% of the CO_{2eq} emissions can be allocated to the crushing process (electricity usage) and only 18% to the mining process (diesel consumption) since the raw material can be easily extracted on the earth's surface. For the production of sodium nitrate, about 42% of the overall manufacturing GHG emissions (0.05 kgCO_{2eq}/kg) are related to the heat requirements, respectively the natural gas consumption.

In the production of mined potassium chloride (Figure 25), the largest contributor to manufacturing GHG emissions, at 83%, is the vinyl material used in the plastic-lined

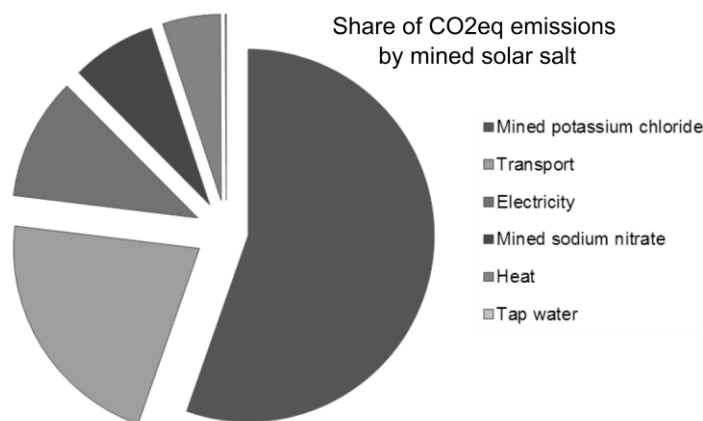
evaporation ponds, followed by the Salar brine extraction (diesel consumption and electricity usage) at approx. 10%.

Figure 25: Share of CO_{2eq} emissions by mined potassium chloride from SQM, Chile. The overall GHG emissions are estimated to generate 0.48 kgCO_{2eq}/kg.



In the manufacturing GHG emissions of solar salt Figure 26, potassium chloride is the primary contributor with 55%, followed by transportation from Chile to Spain at 22%, and sodium nitrate production at only 7%.

Figure 26: Share of CO_{2eq} emissions from the manufacturing process by mined solar salt at SQM, Chile. This process includes the crystallization from sodium nitrate and potassium chloride to the favorable mix of sodium nitrate (60 wt%) and potassium nitrate (40 wt%).



Overall, mined solar salt is estimated to generate GHG emissions (manufacturing including transport) of approx. 0.86 kgCO_{2eq}/kg. When compared to the CO_{2eq} emissions in the synthetic production of solar salt via nitric acid (3.8 kgCO_{2eq}/kg), estimated from Ecoinvent 3.3 background data for sodium nitrate and potassium nitrate, the usage of mined solar salt in TES systems is highly preferable from an environmental point of view.

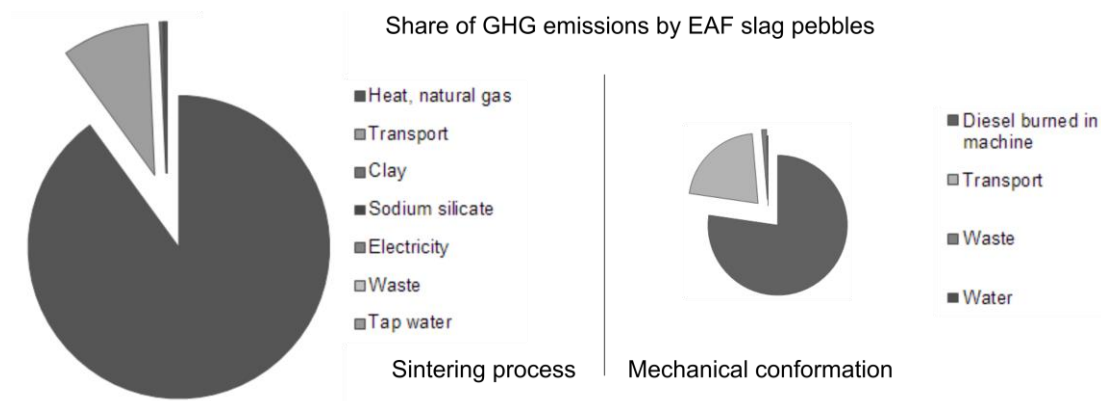
6.2 EAF slag filler material

As detailed in chapter 2.3.2, two manufacturing pathways for the EAF slag pebbles were investigated in this work: the sintering process and the mechanical

conformation process (Figure 27). Compared to mechanical conformation, the sintering process is estimated to increase manufacturing GHG emissions by 56%. This is mainly due to the heat requirement associated with natural gas consumption by the sintering furnace (0.58 kgCO_{2eq}/kg). The contributions from the binder material (clay, sodium silicate), the electricity usage, the waste handling, and the tap water consumption are negligible (0.7%).

The GWP for the mechanical conformation process relating to diesel consumption is estimated at approx. 0.22 kgCO_{2eq}/kg. The estimated GHG emissions for the waste handling and water consumption contribution are estimated at about 1% only.

Figure 27: Share of CO_{2eq} emissions from the manufacturing process by EAF slag pebbles via the sintering process and via the mechanical conformation. The amount of estimated GHG emissions from the sintering process is more than double (0.64 kgCO_{2eq}/kg) compared to the mechanical conformation method (0.28 kgCO_{2eq}/kg). The illustration ratio between both methods is 1:1.



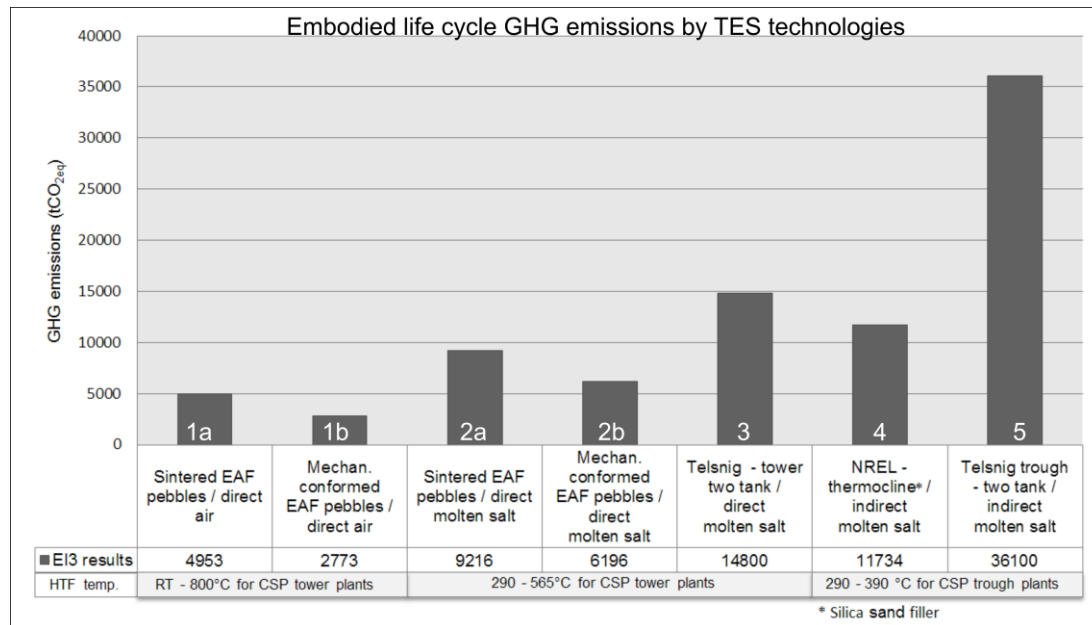
Transportation for both methods was assumed to be the same (0.06 kgCO_{2eq}/kg), resulting in a contribution of approx. 9% from the sintering process and 21% from the mechanical conformation method.

6.3 Embodied life-cycle GHG emissions by TES systems

Figure 28 summarizes the results of the evaluation of EAF slag-based packed bed storage systems (systems 1a, 1b, 2a, 2b) and comparable alternative TES technologies (system 3, 4, 5) as listed in Figure 17. All results are based on the embodied emissions of GHGs from the material and energy required to supply 6 hours of thermal storage for 50 MWe CSP plants. The GHG emissions of the conventional two-tank indirect molten solar salt (system 5) are estimated to be approx. 36'100 tCO_{2eq}. Analogous GHG emissions for the thermocline system with quartzite rock and silica sand as a filler material (system 4) are almost 60% lower. This strong reduction can be mainly associated with the reduced requirements for the solar salt inventory and the much lower GHG emission contribution from the filler

material. The material savings result from the fact that only a single tank is necessary for the thermocline system.

Figure 28: Comparison of the embodied life-cycle GHG emissions from materials used in indirect and direct two-tank and thermocline molten solar salt and air TES systems designed to supply 6 hours of thermal storage for 50 MWe CSP plants.



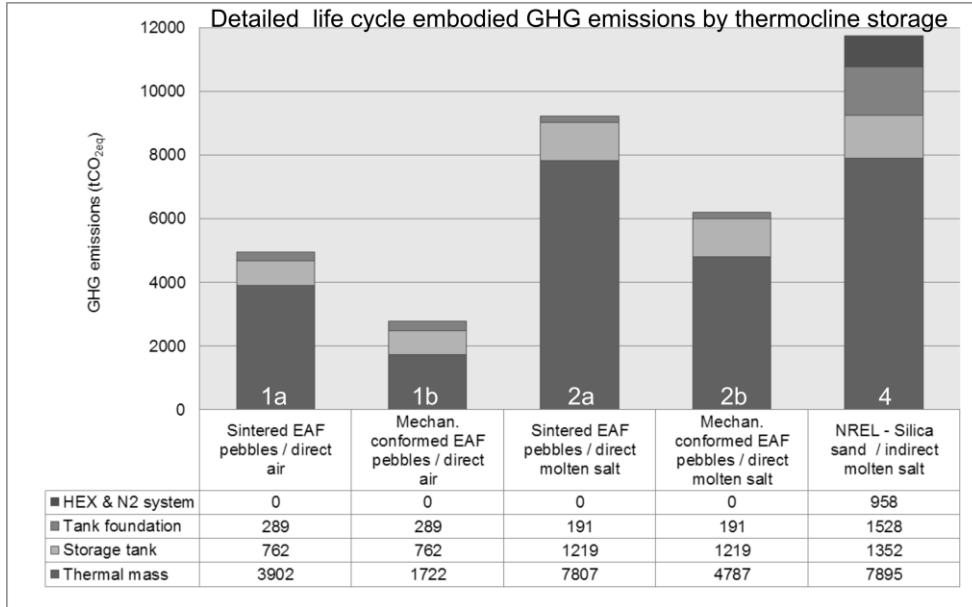
Total embodied GHG emissions show a positive trend for the TES systems with an increased HTF operation temperature range. For example, system 3 (two-tank direct molten salt storage) is estimated to decrease embodied GHG emissions by 67% when compared to system 5 (two-tank indirect molten salt storage). This effect demonstrates the significance of higher operating temperatures and the direct implementation of a TES system that eliminates the need for additional heat exchanger hardware.

The EAF slag-based packed bed storage alternatives (system 1 and 2) show further improved embodied GHG emissions due to the additional reduction of the solar salt inventory and its increased replacement by EAF slag pebbles material. It also indicates a clear advantage in the use of the mechanical conformed pebbles (system 1b, 2b).

Figure 29 shows the detailed environmental impacts of the components of the thermocline storage options (system 1, 2, 4). Substituting molten solar salt with air decrease life-cycle embodied GHG emissions by 46% when using the sintered EAF pebbles as a filler material or 55% for the mechanical conformed EAF slag pebbles. One fourth of this reduction can be also linked to the optimized thermocline tank

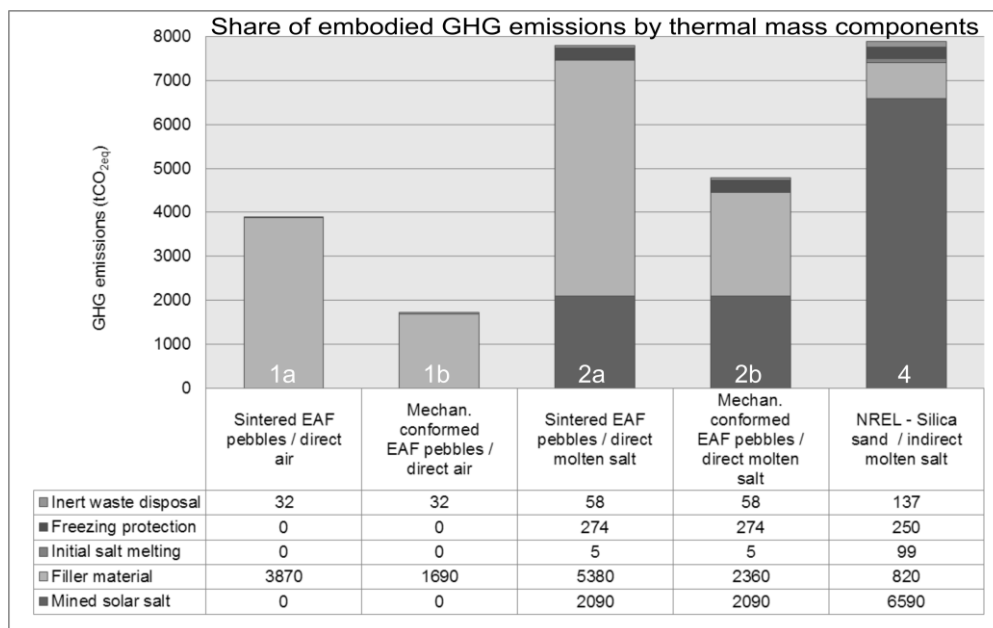
design which has smaller tank volume requirements when operated with air as a HTF (system 1).

Figure 29: Comparison of the embodied GHG emissions from materials and energy used in the thermocline storage systems.



For all thermocline systems, the thermal mass component is the primary contributor, representing 62 – 85%. Further details of the thermal mass inventory and its contribution to the total embodied GHG emissions are shown in Figure 30. It highlights the extent of CO_{2eq} emissions from the thermal mass component which depends on the material mass ratio of the HTF and the filler material.

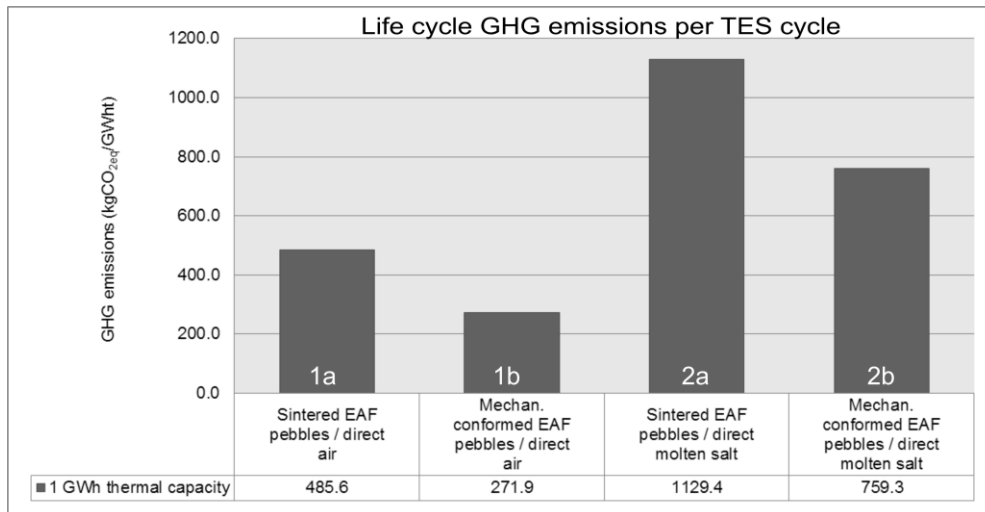
Figure 30: Share of CO_{2eq} emissions by thermal mass component from materials and energy used in the thermocline storage systems.



For the molten solar salt-based thermocline storage options (system 2 and 4), additional embodied GHG emissions associated with the initial salt melting and freezing protection account for approx. 5%.

Figure 31 presents the results of estimated life-cycle GHG emissions assuming a lifetime of 30 years and a discharge rate of 340 per year for system 1 and 2, leading to an overall capacity output of 10'200 GWht for system 1 and 8'160 GWht for system 2. The resulting life-cycle environmental impact per discharge (1 GWht) ranges from approx. 272 to 1'130 kgCO_{2eq}/GWht.

Figure 31: Life-cycle GHG emissions of the EAF slag-based thermocline TES storage. The functional unit represents a 1 GWht thermal storage capacity for a 50 MWe CSP central receiver plant located in Seville, Spain. A lifetime of 30 years and a yearly discharging rate of 340 are assumed.



For both configurations, the estimated CO_{2eq} emissions per kWh electricity output related to the TES system can be calculated via the steam turbine efficiency (40% for system 1, 30% for system 2) as indicated in Table 3. The resulting life-cycle GHG emissions of the EAF slag-based packed bed systems per electricity output generated, *from the thermal storage systems only*, are reported in Table 10.

Table 10: Life-cycle GHG emissions for the EAF slag-based packed bed TES systems per electricity output from the stored thermal capacity.

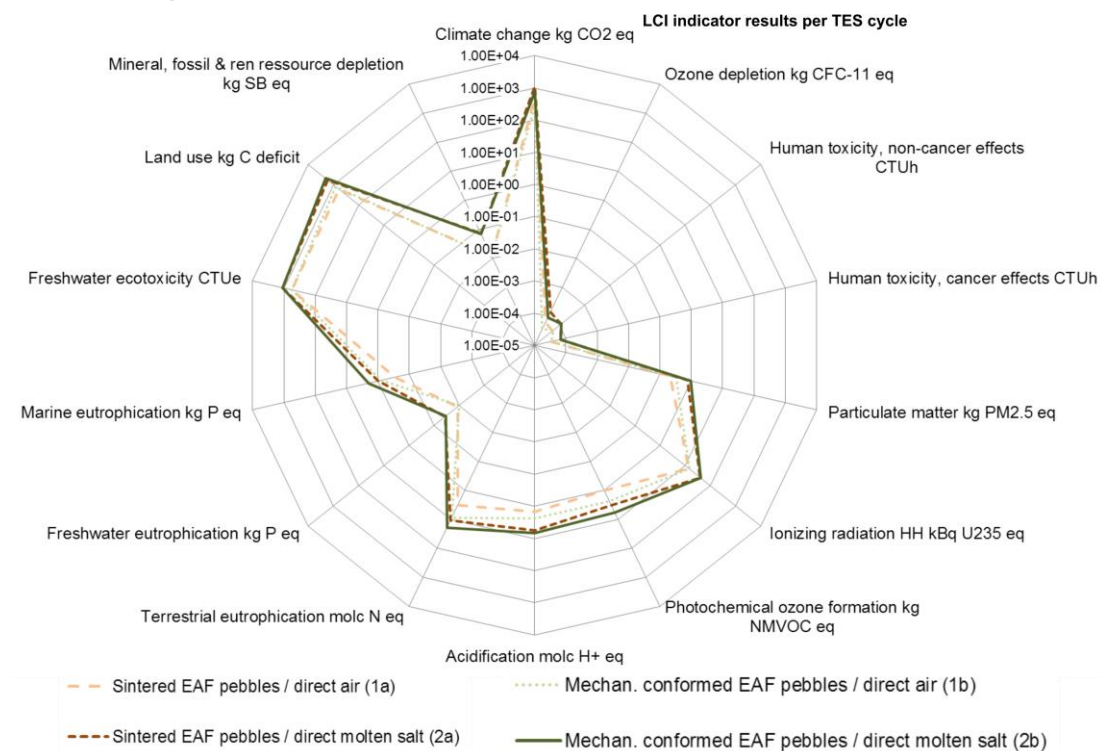
Thermocline storage	System 1a	System 1b	System 2a	System 2b
gCO _{2eq} emissions per kWhe output	1.62	0.91	3.53	2.37

The overall estimated contribution of GHG emissions from the EAF slag-based thermocline storage systems are below 4 gCO_{2eq}/kWhe. If air is used (system 1a, or b) instead of molten solar salt (system 2a, or b) as an HTF, life-cycle GHG emissions are estimated to be lower by 54 to 74%. Using the mechanical

conformation (pathway b) over the sintering process (pathway a) lowers life-cycle GHG emissions by 44%, in the case of the air-based system 1, and 33% within the molten solar salt system 2. However, the production of pebbles via the sintering pathway leads to favorable spherical shapes and more accurate pebble dimensions when compared to mechanical conformation, as described in chapter 2.3.2. In either case, these results assume that the EAF slag pebbles do not need to be replaced and are able to withstand operation for the complete lifetime of 30 years. Therefore, it is important to confirm the technical feasibility and efficiency assumptions for both production pathways performed within the Slagstock project WP4.

In addition to the results on GHG emissions, further LCIA indicators are presented in Figure 32. Land use for the air-based thermocline systems (1a, 1b) is estimated to improve environmental impacts by 35 – 38% compared to molten salt-based TES system (2a, 2b). In contrast to the results on life-cycle GHG emissions, where the air-based system 1b (mechanical conformed pebbles) shows the best results, the EAF slag-based packed bed system 1a (sintered pebbles) is estimated to have similar or better values for other LCI indicators.

Figure 32: LCIA results of the EAF slag-based thermocline TES storage based on the functional unit of 1 GWht with a lifetime of 30 years and a yearly discharging rate of 340. The indicators are based on the recommendation by Hauschild et al. (2013). The graphic shows the results based on a \log_{10} scale.

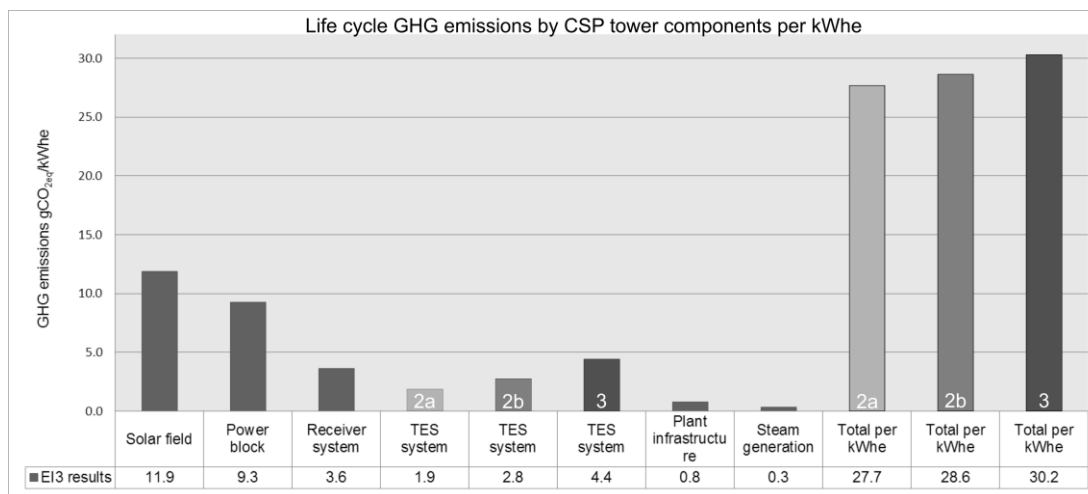


In general, the thermocline system using the sintered EAF slag pebbles (system 1a, 2a) is estimated to have slightly improved life-cycle environmental impacts for some indicators. This trend is caused by the thermal mass component of the TES system and may result from the mechanical conformation via an open air tumbling process and its creation of dust which is not filtered and also from the diesel burned in the combustion engine of the vehicle (at this development stage), as mentioned in chapter 2.3.2. However, the creation of particles (0.04 kg per kg of EAF slag pebbles production) during the tumbling process could not be measured and is an assumption which should be examined further.

6.4 50 MWe CSP central receiver plant including EAF slag-based TES system

The overall environmental performance of STE generation from the CSP tower plant as introduced at the end of chapter 4 is summarized in Figure 33. The results are segmented into the plant components and reveal that the largest contribution of life-cycle GHG emissions (11.9 gCO_{2ep}/kWh_e) is related to the solar field. This effect is mainly caused by the requirements of the large amount of steel (68% of the solar field share) and flat glass (16% of the solar field share) to build the 6'346 heliostats.

Figure 33: Share of life-cycle GHG emissions by CSP tower components for a 50 MWe steam turbine incorporating a 6 hour direct TES system designs located in Seville, Spain. The functional unit is based on 1 kWh_e of electricity production.

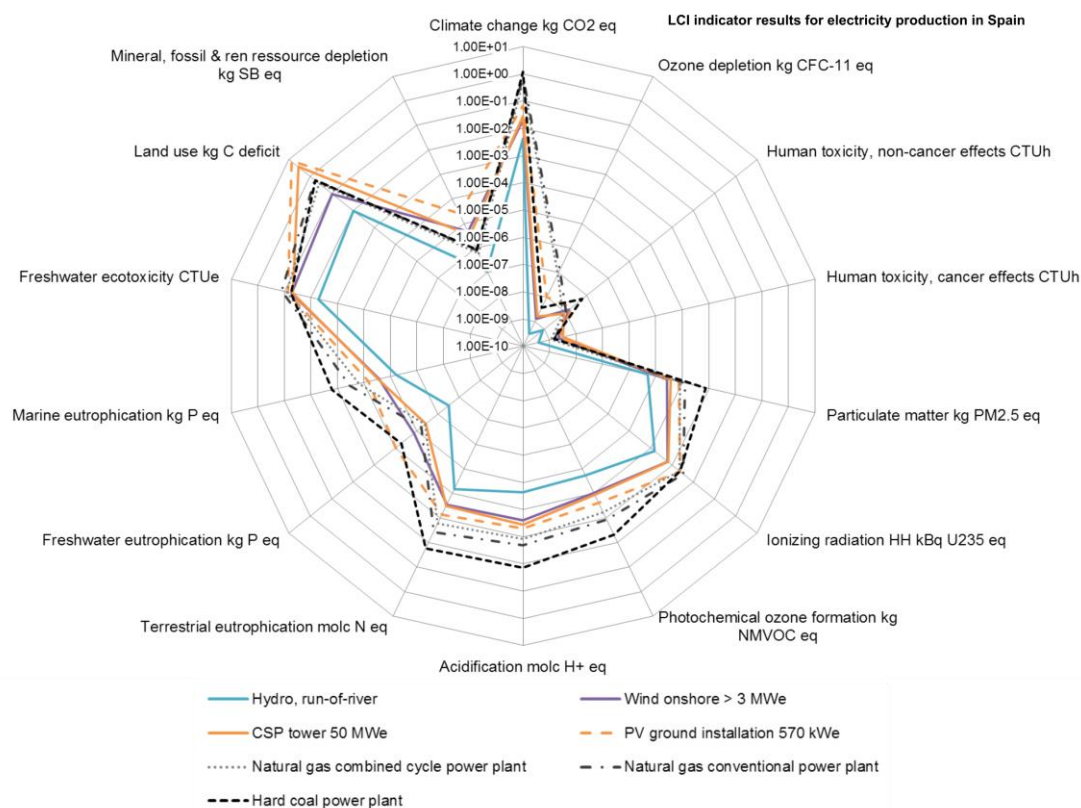


The power block is estimated to generate 9.3 g CO_{2eq}/kWh_e as a consequence of the large amounts of construction material required for the dry cooling tower and the pumps and compressors. Compared to the receiver system, which accounts for approximately 12% of the total life-cycle GHG emissions, the plant infrastructure and steam generation components are estimated to have a rather marginal impact (1 – 3%) only.

Design configurations for the direct molten solar salt TES systems are the two-tank (system 3) and the thermocline EAF slag pebbles designs (2a, and 2b). The switch to a thermocline system decreases TES related life-cycle GHG emissions by a minimum of approximately 38% or even up to 58% depending on the environmental impact of the thermocline filler material. Therefore, the total amounts of life-cycle GHG emissions range from 27.7 – 30.2 g CO_{2eq}/kWh, which is similar to the results published by LCAs on CSP tower plants (Whitaker, et al., 2013), (Burkhardt, Heath, & Cohen, 2012), (Lechon, de la Rua, & Saez, 2008), see Figure 2.

When putting CSP in perspective with alternative renewable and non-renewable electricity generation technologies to be used for Spanish electricity supply, the CSP results for most selected LCIA indicators are found to be below fossil fuel-based systems (Figure 34).

Figure 34: Selected life-cycle environmental impacts of current electricity generation systems in Spain (per kWh). The CSP tower plant incorporates the EAF slag-based packed bed system design 2b (mechanical conformation). LCI data of the alternative technologies are selected from the Ecoinvent database 3.3 (Wernet, et al., 2016). The selected LCIA indicators are based on the recommendation by Hauschild et al. (2013). The graphic shows the results based on a log₁₀ scale.



The LCI results for the presented alternative technologies (Spanish specific) are taken directly from the Ecoinvent 3.3 database (Wernet, et al., 2016). The presented

environmental impacts from CSP electricity generation are based on the 50 MWe central receiver plant incorporating the thermocline TES system 2b (mechanical conformed EAF slag pebbles) which is estimated to create similar environmental effects compared to onshore wind turbines (>3 MWe) for several LCI indicators.

It is obvious that the land usage of CSP and PV (ground installation) systems are significantly larger compared to other technologies. It is important to note though, that the most suitable locations for CSP systems are deserts and arid, unused, non-agricultural land.

7 SUMMARY AND CONCLUSIONS

The reported LCA results represent a comparative, bottom-up assessment of life-cycle GHG emissions and selected LCIA indicators of various TES systems for CSP applications. Furthermore, the environmental burdens and potential impacts of a 50 MWe CSP tower plant located in southern Spain were evaluated and compared with other renewable and non-renewable electricity generation to be used for the Spanish electricity supply.

In general, environmental impacts of STE production from solar-only CSP plants vary depending on the technology used and plant location (solar irradiance). The estimated life-cycle GHG emissions of 27.7 – 30.2 g CO_{2eq}/kWh_e for the CSP tower plant remain as expected within the reported range by Burkhard et al. (2012) (5-60 gCO_{2eq}/kWh_e). These results confirm that this renewable technology can provide electricity with life-cycle GHG emissions on par with other renewables technologies and are significantly lower when compared to life-cycle GHG emissions from natural gas or coal generation by approx. 97%. Additionally, for most LCI indicators, the estimated environmental impacts of STE production are comparable to wind turbines. However, greater land consumption is the main environmental consequence for CSP systems.

A major advantage of CSP technology is the ability to integrate large thermal storage systems in order to generate electricity beyond the daytime sun hours and provide dispatchability options. This characteristic makes CSP plants competitive and complementary to PV systems. New CSP tower plants, like the 110 MWe Atacama STE plant in Chile, incorporating 15 – 17.5 hours of thermal storage (molten solar salt as HTF and storage material), and are able to operate as a solar-only baseload facility, further improving capacity factors and levelised costs. The thermal storage system, therefore, is a key component of CSP technologies.

One option to reduce the environmental impact of TES systems is to increase the temperature differential of the HTF across the storage system by applying CSP tower configurations (system 1 – 3, Figure 17) rather than using CSP trough designs (system 4 and 5). This allows for a direct implementation of the TES system, thus eliminating the need for an additional heat exchanger. Furthermore, this increases thermal storage density and decreases the amount of storage material required, resulting in a reduction in life-cycle GHG emissions by approx. 60% (system 3 instead of system 5).

More detailed results on life-cycle GHG emissions of common utility-scale molten solar salt TES systems (system 2 – 5) reveal that a substantial contribution is derived from the thermal mass component (solar salt and storage material) caused mainly by the large amounts of storage material required. This fact stresses the importance of assessing the environmental impact of the storage material used in the TES system. Consequently a detailed examination of the solar salt manufacturing GHG emissions was performed. The results show that the usage of mined solar salt as an HTF is highly preferable from an environmental point of view as opposed to synthetically produced solar salt.

In general, switching to thermocline packed bed system designs (from system 5 to 4 or from system 3 to 2) can further aid in mitigating increased impacts from the solar salts due to the partial replacement of the salt inventory with a filler material. However, this effect highly depends on the environmental burdens of the filler material.

The detailed assessment of using EAF slag as a filler material in a thermocline packed bed system estimated that life-cycle GHG emissions can be reduced by approx. 38% when producing the EAF slag pebbles via the sintering process (system 2a) or even 58% via mechanical conformation (system 2b) when compared to a direct two-tank TES system (system 3). For both pebble manufacturing pathways, energy consumption (natural gas, diesel) is the primary contributor to life-cycle GHG emissions.

With respect to some other environmental performance indicators (e.g. particulate matter, acidification, and marine eutrophication), the EAF slag pebble sintering process (pathway a) is estimated to have slightly improved environmental impacts. This effect appears to result from an up to now rather improvised tumbling process (via an industrial concrete mixer) and the creation of a noticeable amount of dust. Therefore, the mechanical conformation process (pathway b) should be improved, for example, by using closed industrial rock tumbler machines to capture or filter slag particles.

With this in mind, applying an improved mechanical conformation process (pathway b) for future industrial manufacturing of the EAF slag pebbles is preferable from an environmental point of view. However, it is important to note that all estimated results assume that the EAF slag pebbles are able withstand operation of the complete lifetime (30 years) and do not need to be replaced. This is an assumption

that still needs to be confirmed by the technical assessment performed in the Slagstock project.

In case replacement of the pebbles is required, one complete exchange of EAF slag pebbles produced via the sintering process (pathway a) will increase life-cycle GHG emissions to almost the same level as that from a direct two-tank molten solar salt TES configuration (system 3). For the mechanical conformation method (pathway b), four complete replacements raise life-cycle GHG emissions to just below the amount of the two-tank storage design.

It should be also noted that the sintering process (pathway a) produces pebbles with more favorable characteristics (spherical shape and dimension) from an efficiency point of view. This might slightly influence the environmental performance of the TES system. Therefore, the technical efficiency of both pathways (sintering process and mechanical conformation) of the EAF slag pebbles will be investigated in the pilot plant tests within the Slagstock project.

An alternative HTF for future CSP technologies can be air, making even higher operating temperatures possible and eliminating the necessity of solar salt entirely. In this case, the EAF slag-based thermocline storage design (system 1b) is estimated to further reduce life-cycle GHG emissions to 0.91 gCO_{2eq}/kWh of electricity stored, as opposed to 2.37 gCO_{2eq}/kWh for the molten salt EAF slag thermocline system 2b.

As repeatedly pointed out however, the TES system is only one component of a CSP system and it is therefore necessary to include all components of the complete air-based CSP plant in the LCA in order to evaluate the entire environmental burdens of this CSP application. Unfortunately, due to the lack of literature for the less mature CSP volumetric air receiver system, it was not possible to evaluate the promising alternative further within this Master's Thesis. Therefore, additional research is necessary to complete the LCA on the air-based CSP system and confirm environmental improvements for the whole CSP system.

Furthermore, additional components (i.e. solar field, receiver system, steam generation, power block, and plant infrastructure) of the evaluated molten solar salt CSP tower system 2 are based on an available hypothetical reference system design engineered by Abengoa Solar. Therefore it is recommended to update this comparison as new design estimates emerge.

REFERENCES

- Adeoye, J. T., Amha, Y. M., Poghosyan, V. H., Torchyan, K., & Arafat, H. a. (2014). Comparative LCA of Two Thermal Energy Storage Systems for Shams1 Concentrated Solar Power Plant: Molten Salt vs. Concrete. *Journal of Clean Energy Technologies*, 2(3), 274-281. doi:10.7763/JOCET.2014.V2.139
- Bauer, C., Hirschberg (eds.), S., Bäuerle, Y., Biollaz, S., Calbry-Muzyka, A., Cox, B., . . . Tran, M. (2017). *Potentials, costs and environmental assessment of electricity generation technologies*. PSI, WSL, ETHZ, EPFL, Paul Scherrer Institut, Villigen PSI, Switzerland.
- Breidenbach, N., Martin, C., Jockenhöfer, H., & Bauer, T. (2016). Thermal Energy Storage in Molten Salts: Overview of Novel Concepts and the DLR Test Facility TESIS. *Energy Procedia*, 99, 120-129. doi:10.1016/j.egypro.2016.10.103
- Brosseau, D. A., Hlava, P. F., & Kelly, M. J. (2005). Testing Thermocline Filler Materials and Molten Salt Heat Transfer Fluids for Thermal Energy Storage Systems Used in Parabolic Trough Solar Power Plants. *Solar Energy Eng-Trans ASME*, 127, 109-1016. doi:10.1115/ISEC2004-65144
- Bureau of International Recycling. (2017). *World Steel Recycling in Figures 2012-2016*. Ferrous Division, Brussels, Belgium.
- Burgaleta, J. I., Arias, S., & Ramirez, D. (2011). GEMASOLAR, the First Tower Thermosolar Commercial Plant With Molten Salt Storage. Granada, Spain: Proceedings of the SolarPACES Conference on Concentrated Solar Power and Chemical Energy Systems.
- Burkhardt, J., Heath, G. A., & Cohen, E. (2012). Life Cycle Greenhouse Gas Emissions of Trough and Tower Concentrating Solar Power Electricity Generation. *Journal of Industrial Ecology*, 16(S1), S93-S109.
- Calvet, N., Gomez, J., Faik, A., Roddatis, V., Meffre, A., Glatzmaier, G., . . . Py, X. (2013). Compatibility of a post-industrial ceramic with nitrate molten salts for use as filler material in a thermocline storage system. *Applied Energy*, 109, 387-393. doi:10.1016/j.apenergy.2012.12.078
- Casubolo, G. (2017, Juli 17). Personal communication. SQM.

- Chang, Z., Li, A., Xu, C., Chang, C., & Wang, Z. (2015). The design and numerical study of a 2MWh molten salt thermal tank. *Energy Procedia*, 69, 779-789. doi:10.1016/j.egypro.2015.03.094
- Dobos, A., Neises, T., & Wagner, M. (2014). Advances in CSP simulation technology in the System Advisor Model. *Energy Procedia*, 49, 2482 – 2489. doi:10.1016/j.egypro.2014.03.263
- EC. (2010). *International Reference Life Cycle Data System (ILCD) Handbook - General guide for Life Cycle Assessment - Detailed guidance*. Luxembourg: European Commission, Joint Research Centre, Institute for Environment and Sustainability.
- European Academies Science Advisory Council, easac. (2011). *Concentrating solar power: its potential contribution to a sustainable energy future*. Halle, Germany.
- EUROSLAG – The European Slag Association. (2017, September 12). Retrieved from Products - EAF: <http://www.euroslag.org>
- Fasquelle, T., Falcoz, Q., Neveu, P., Lacat, F., Boulet, N., & Flamant, G. (2017). Operating Results of a Thermocline Thermal Energy Storage Included in a Parabolic Trough Mini Power Plant. 1850, pp. 080010-1–080010-8. AIP Conference Proceedings. doi:10.1063/1.4984431
- Flueckiger, S., Yang, Z., & Garimella, S. V. (2011). An integrated thermal and mechanical investigation of molten-salt thermocline energy storage. *Applied Energy*, 88(6), 2098-2105. doi:10.1016/j.apenergy.2010.12.031
- Fondriest Environmental, Inc. (2017, September 15). *Solar Radiation and Photosynthetically Active Radiation*. Retrieved from Fundamentals of Environmental Measurements: <http://www.fondriest.com/environmental-measurements/parameters/weather/solar-radiation/>
- Gabrielli, R., & Zamparelli, C. (2009). Optimal design of a molten salt thermal storage tank for parabolic trough solar power plants. *J. Sol. Energy Eng*, 131(4), 0410011-04100110. doi:10.1115/1.3197585
- Gil, A., Medrano, M., Martorell, I., Lázaro, A., Dolado, P., Zalba, B., & Cabeza, L. (2010). State of the art on high temperature thermal energy storage for power generation. Part 1—Concepts, materials and modellization. *Renewable and Sustainable Energy Reviews*, 14(1), 31-55. doi:10.1016/j.rser.2009.07.035

- Hasnaina, S. M. (1998). Review on sustainable thermal energy storage technologies. Part 1. Heat storage materials and techniques. *Energy Conversion and Management*, 39(11), 1127-1138. doi:10.1016/S0196-8904(98)00025-9
- Hauschild, M., Goedkoop, M., Guinée, J., Heijungs, R., Huijbregts, M., Jolliet, O., . . . Pant, R. (2013). Identifying best existing practice for characterization modeling in life cycle impact assessment. *The International Journal of Life Cycle Assessment*, 18(3), 683-697. doi:10.1007/s11367-012-0489-5
- Heath, G., Turchi, C., Burkhardt, J., Kutscher, C., & Decker, T. (2009). Life cycle assessment of thermal energy storage: Two-tank indirect and thermocline. San Francisco, USA: ASME 2009 3rd International Conference on Energy Sustainability.
- Hennecke, K., Schwarzbözl, P., Koll, G., Beuter, M., Hoffschmidt, B., Götttsche, J., & Hartz, T. (2008). The Solar Power Tower Jülich — A Solar Thermal Power Plant for Test and Demonstration of Air Receiver Technology. *ISES World Congress, Vol. 1 - Vol. V*, pp. 1749-1753. doi:10.1007/978-3-540-75997-3_358
- Houston, J., Butcher, A., Ehren, P., Evans, K., & Godfrey, L. (2011). The Evaluation of Brine Prospects and the Requirement for Modifications to Filing Standards. *Economic Geology*, 106(7), 1225-1239. doi:10.2113/econgeo.106.7.1225
- IEA. (2014). *Technology Roadmap: Solar Thermal Electricity*. OECD/IEA, Paris.
- IPCC. (2013). *Climate Change 2013: The Physical Science Basis. Working Group I contribution to the Fifth Assessment Report of the IPCC*. Geneva, Switzerland: Intergovernmental Panel on Climate Change, IPCC.
- ISO 14040. (2006). Environmental management - Life cycle assessment - Principles and framework. Retrieved from <https://www.iso.org/obp/ui/#iso:std:iso:14040:ed-2:v1:en>
- ISO 14044. (2006). Environmental management - Life cycle assessment - Requirements and guidelines. Retrieved from <https://www.iso.org/obp/ui/#iso:std:38498:en>
- Kearney, D., Herrmann, U., Nava, P., Kelly, B., Mahoney, R., Pacheco, J., . . . Price, H. (2003). Assessment of a Molten Salt Heat Transfer Fluid in a Parabolic

- Trough Solar Field. *Journal of Solar Energy Engineering*, 125(2), 170-190.
doi:10.1115/1.1565087
- Kelly, B. (2005). *Nexant Parabolic Trough Solar Power Plant Systems Analysis*. San Francisco, USA: National Renewable Energy Laboratory, NREL.
- Kelly, B. (2010). *Advanced Thermal Storage for Central Receivers with Supercritical Coolants*. Lakewood, USA: Abengoa Solar Inc.
- Kelly, B., & Kearney, D. (2006). *Thermal storage commercial plant design for a 2-tank indirect molten salt system*. National Renewable Energy Laboratory. Retrieved from www.nrel.gov/docs/fy06osti/40166.pdf
- Klein, S., & Rubin, E. (2013). Life cycle assessment of greenhouse gas emissions, water and land use for concentrated solar power plants with different energy backup systems. *Energy Policy*, 63, 935-950.
doi:10.1016/j.enpol.2013.08.057
- Kogel, J., Trivedi, N., Barker, J., & Krukowski, S. (2006). *Industrial Minerals & Rocks: Commodities, Markets, and Uses*. Littleton, USA: Society for Mining, Metallurgy, and Exploration, Inc.
- Kuravi, S., Goswami, D., Stefanakos, E., Manoj, R., Jotshi, C. P., Traha, J., . . . Krakow, B. (2012). Thermal energy storage for concentrating solar power. *Technology and Innovation*, 14, 81-91.
doi:10.3727/194982412X13462021397570
- Kuravi, S., Trahan, J., Goswami, D. Y., Rahman, M. M., & Stefanakos, E. K. (2013). Thermal energy storage technologies and systems for concentrating solar power plants. *Progress in Energy and Combustion Science*, 39, 285-319.
doi:10.1016/j.pecs.2013.02.001
- Laing, D., Steinmann, W.-D., Tamme, R., & Richter, C. (2006). Solid media thermal storage for parabolic trough power plants. *Solar Energy*, 80, 1283-1289.
doi:10.1016/j.solener.2006.06.003
- Lalau, Y., Py, X., Meffre, A., & Olives, R. (2016). Comparative LCA between current and alternative waste-based TES for CSP. *Waste and Biomass Valorization*, 7(6), 1509-1519. doi: 10.1007/s12649-016-9549-6
- Lechon, Y., de la Rua, C., & Saez, R. (2008). Life Cycle Environmental Impacts of Electricity Production by Solarthermal Power Plants in Spain. *Journal of Solar Energy Engineering*, 120(2). doi:10.1115/1.2888754

- Libby, C. (2010). *Solar Thermocline Storage Systems: Preliminary Design Study*. ELECTRIC POWER RESEARCH INSTITUTE. Palo Alto, CA: EPRI.
- Libby, C., & Key, T. (2009). *Program on technology innovation: evaluation of concentrating thermal energy storage systems*. Palo Alto, USA: Electric Power Research Institute, USA.
- Mira-Hernandez, C., Flueckiger, S., & Garimella, S. (2015). Comparative analysis of single- and dual-media thermocline tank for thermal energy storage in concentrating solar power plants. *ASME. J. Sol. Energy Eng.*, 137(3). doi:10.1115/1.4029453
- Modi, A., & Perez-Segarra, C. (2014). Thermocline thermal storage systems for concentrated solar power plants: Onedimensional numerical model and comparative analysis. *Solar Energy*, 100, 84-93. doi:10.1016/j.solener.2013.11.033
- Muñoz-Sánchez, B., Iparraguirre-Torres, I., Madina-Arrese, V., Unzurrunzaga-Iturbe, A., & García-Romero, A. (2015). Encapsulated high temperature PCM as active filler material in a thermocline-based thermal storage system; Izagirre-Etxeberria, U.; *Energy Procedia*, 69, 937-946. doi:10.1016/j.egypro.2015.03.177
- Oró, E., Gil, A., de Gracia, A., Boer, D., & Cabeza, L. (2012). Comparative life cycle assessment of thermal energy storage systems for solar power plants. *Renewable Energy*, 44, 166-173. doi:10.1016/j.renene.2012.01.008
- Ortega, I., Faik, A., Gil, A., Rodrigues-Aseguinolaza, J., & D'Aguanno, B. (2014). Thermo-physical properties of a steel-making by-product to be used as thermal energy storage material in a packed-bed system. *International Conference on Concentrating Solar Power and Chemical Energy Systems, SolarPACES* (pp. 968-977). Beijing, China: Energy Procedia. doi:10.1016/j.egypro.2015.03.180
- Ortega-Fernandez, I., Calvet, N., Gil, A., Rodríguez-Aseguinolaza, J., Abdessamad, F., & D'Aguanno, B. (2015). Thermophysical characterization of a by-product from the steel industry to be used as a sustainable and low-cost thermal energy storage material. *Energy*, 89, 601-609. doi:10.1016/j.energy.2015.05.153

- Ortega-Fernandez, I., Lorono, I., Faik, A., Uriz, I., Rodriguez-Aseguinolaza, J., & D'Aguaño, B. (2016). Parametric Analysis of a Packed Bed Thermal Energy Storage System. *AIP Conf. Proc.*, 080021-1-8. doi:10.1063/1.4984442
- Pacheco, J. E. (2002). *Final Test and Evaluation Results from the Solar Two Project*. Albuquerque, USA: Solar Thermal Technology.
- Pacheco, J. E., Showalter, S. K., & Kolb, W. J. (2002). Development of a Molten-Salt Thermocline Thermal Storage System for Parabolic Trough Plants. *Journal of Solar Energy Engineering*, 124(2), 153-159.
- Sallaberry, F., De Jalón, A. G., Zaversky, F., Vázquez, A. J., López-Delgado, A., Tamayo, A., & Mazo, M. A. (2015). Towards Standard Testing Materials for High Temperature Solar Receivers. *Energy Procedia*, 532-542. doi:10.1016/j.egypro.2015.03.062
- Siegel, N. (2012). Thermal energy storage for solar power production. *WIREs Energy Environ*, 1, 119-131. doi:10.1002/wene.10
- Siemens AG. (2010). *Steam turbines for CSP plants*. Erlange, Germany: Siemens AG, energy Sector. Retrieved from www.siemens.com/energy
- SimaPro v8.3*. (2017). The Netherlands: <http://www.pre.nl/simapro/>.
- Singh, H., Saini, R., & Saini, J. (2010). A review on packed bed solar energy storage systems. *Renewable and Sustainable Energy Reviews*, 1059-1069. doi:10.1016/j.rser.2009.10.022
- Solar Millenium. (2008). *The parabolic trough power plants Andasol 1 to 3 - The largest solar power plants in the world*. Retrieved September 26, 2017, from www.solarmillennium.de
- SQM. (2016). *Sustainability report*. Santiago, Chile: SQM, El Trovador 4285. Retrieved 10 2017, from <http://ir.sqm.com/English/investor-relation/Annual-information/default.aspx>
- SQM. (2017). *Thermo-Solar Salts*. Retrieved 09 10, 2017, from <http://www.sqm.com/en-us/productos/quimicosindustriales/salestermo-solares.aspx>
- Telsnig, T. (2015). *Location-specific analysis and assessment of solar thermal power plants in South Africa*. University of Stuttgart, Germany. doi:10.18419/opus-2384

- Teske, S. (2016). *Global Solar Thermal Electricity Outlook 2016*. Amsterdam, Netherlands: European Solar Thermal Power Industry Association (ESTIA), IEA SolarPACES and Greenpeace International.
- Trieb, F., Schillings, C., O'Sullivan, M., Pregger, T., & Hoyer-Klick, C. (2009). Global Potential of Concentrating Solar Power. *SolarPaces Conference*. Berlin, Germany.
- Wernet, G., Bauer, C., Steubing, B., Reinhard, J., Moreno-Ruiz, E., & Weidema, B. (2016). The ecoinvent database version 3 (part I): overview and methodology. *The International Journal of Life Cycle Assessment, [online]*, 21(9), 1218-1230. doi:10.1007/s11367-016-1087-8
- Whitaker, M., Heath, G., Burkhardt, J., & Turchi, C. (2013). Life Cycle Assessment of a Power Tower Concentrating Solar Plant and the Impacts of Key Design Alternatives. *Environmen. Sci. Technol.*, 5896-5903. doi:10.1021/es400821x
- Wieckert, C. (2017, July 10). Personal communication. *PSI*. Villigen.
- Yang, Z., & Garimella, S. V. (2010). Thermal analysis of solar thermal energy storage in a molten-salt thermocline. *Solar Energy*, 84(6), 974-985. doi:10.1016/j.solener.2010.03.007
- Zanganeh, G., Pretti, A., Zavattoni, S., Barbato, M., & Steinfeld, A. (2012). Packed-bed thermal storage for concentrated solar power – Pilot-scale demonstration and industrial-scale design. *Solar Energy*, 86, 3084–3098. doi:10.1016/j.solener.2012.07.019
- Zhang, K., Liu, J., Liu, W., & Yang, J. (2011). Preparation of glass–ceramics from molten steel slag using liquid–liquid. *Chemosphere*, 85(4), 689–692. doi:10.1016/j.chemosphere.2011.07.005

APPENDIX A: LIST OF FIGURES

- Figure 1: Concentrating solar technology can only use part of the solar radiation, the direct irradiation. Parabolic shaped mirrors focus this light creating high temperatures which can be used to drive a steam engine. 5
- Figure 2: Life cycle GHG emissions of current electricity generation technologies (at the power plant). Ranges reflect variability in terms of site-conditions, technology specification, and fuel characteristics. Combined heat and power generation in CHP units and fuel cells is allocated according to exergy content of heat and electricity. Data availability for biomass is limited. NG: natural gas; CC: combined cycle; CHP: combined heat and power; LHP: large hydropower; SHP: small hydropower; CSP: concentrated solar power; PV: photovoltaics; EGS: enhanced geothermal systems; CCS: carbon capture and storage; "coal" includes hard coal and lignite. (Bauer, et al., 2017) 7
- Figure 3: Schematics of CSP Technologies (SolarPACES 2016a). Examples of commercial parabolic troughs are the 354 MW_e SEGS plants in California (constructed in 1985-91) and the 280 MW Solana plant in Arizona (2013); Fresnel reflector systems are operational in Spain as 1.4 MW prototype (2009) and 30 MW commercial plant (2012); Solar power towers have been built in California as 10 MW prototype (1996) and 377 MW commercial plant (2013); Parabolic dish prototypes with Stirling engines are being tested in Spain (25 kW modules constructed in 1996-97) and Australia (400 kW big dish erected in 2011) (Bauer, et al., 2017). 9
- Figure 4: Annual solar-to-electricity efficiency as a function of development level for each CSP technology family (European Academies Science Advisory Council, easac, 2011). 11
- Figure 5: Thermal storage and utility demand. STE production with solar-only operation and no thermal storage option show the same characteristics as photovoltaic and wind energy generation, which highly depend on the renewable energy resource. Adding a thermal storage component to a CSP plant allows for extending and/or shifting energy generation to match with peak load demands. 12
- Figure 6: Parabolic trough CSP plant incorporating an indirect molten solar salt storage system. 17
- Figure 7: Central receiver CSP plant incorporating a direct molten solar salt storage system. 18
- Figure 8: Single-tank thermocline TES system. Ideal temperature distribution with no temperature stratification (1) leads to a maximum storage capacity. More realistically, temperature stratification (thermocline layer) forms between the hot and cold section (2). In case of a complete mix and temperature equalization in the tank there is no thermal storage effect (3). 19
- Figure 9: Principle scheme of a thermocline packed bed configuration. A low-cost filler material forms a packed bed inside the tank, and, therefore, allows for the partial replacement of the HTF. The thermocline storage system is charged from the top of the tank, providing fluid flow through the porous bed and the transfer of heat to the filler material. In order to discharge the thermocline system, the fluid flow is reversed. 20

- Figure 10: Process flow diagram of the mining solar salt production at SQM in northern Chile (Atacama Desert). Solar salt is produced using two natural resources, Caliche Ore and Salar brines. After extraction of the raw material, leaching and several crystallization processes form sodium and potassium nitrates. Controlled forming of potassium nitrate is established via the following chemical reaction: $\text{NaNO}_3 + \text{KCl} = \text{KNO}_3 + \text{NaCl}$. An additional final crystallization process then leads to the favorable mix of the solar salt (60 wt% sodium nitrate and 40 wt% potassium nitrate). (SQM, 2017) 23
- Figure 11: Production facilities for the manufacturing process of solar salt in the Atacama Desert, Chile. In (a), the caliche ore extraction is illustrated and (b) shows the evaporation ponds and harvested salt piles from the salar brine. Illustration (c) shows the process plant for the nitrate production. (SQM, 2016) 24
- Figure 12: Flow diagram of the electric-arc-furnace steelmaking process. 25
- Figure 13: EAF slag pebbles produced via the sintering method developed at Tellus Ceram. 27
- Figure 14: Indirect slag melting through a graphite crucible (1500°C) and pebbles pouring into sand moulds during the casting process. 27
- Figure 15: Crushed EAF slag particles (left). An industrial concrete mixer was used to mechanically conform the EAF slag raw material in order to obtain quasi-spherical geometry (right). 28
- Figure 16: Thermocline TES system designs: EAF slag-based with HTF air (system 1) on the left and with HTF molten solar salt (system 2) on the right. The illustration ratio between both packed bed systems is 1:1. 33
- Figure 17: Overview of the LCA TES system comparison. 36
- Figure 18: System boundaries of the life cycle of the EAF slag-based thermocline TES storage solution. The energy and resources requirements for all necessary components and life-cycle stages are considered in order to establish the environmental impact of the investigated TES system. The functional unit represents a 1 GWht thermal storage capacity for a 50 MWe CSP central receiver plant located in Seville, Spain. 36
- Figure 19: Simplified illustration of the complete life cycle for the EAF slag-based packed bed heat storage. It includes resource extraction and manufacturing, transport and construction, operation and maintenance, and dismantling and disposal. The EAF slag is considered to be a pre-consumer scrap. 37
- Figure 20: Simplified illustration of a CSP central receiver plant layout consisting of a solar field, thermocline TES system, steam generator, and power block. The solar energy absorbed by the receiver is used to drive a steam cycle for electricity generation. Depending upon the actual heat demand, excess thermal energy charges a large insulated storage tank, allowing for stable and dispatchable power generation also at times without sunshine. 38
- Figure 21: System boundaries of the life-cycle of a CSP central receiver plant. The energy and resources requirements for all necessary components and life cycle stages are considered in order to establish the environmental impact of the CSP plant. The functional unit represents a 1 kWhe electricity output for a 50 MWe CSP central receiver plant including 6 hours of EAF slag-based thermal storage located in Seville, Spain. 39

Figure 22: Thermocline tank foundation design (Kelly & Kearney, 2006)	41
Figure 23: Overview of the individual TES system application (system 1 – 5) evaluated in this LCA.	47
Figure 24: Share of CO _{2eq} emissions by mined sodium nitrate from SQM, Chile. The overall GHG emissions are estimated to generate 0.05 kgCO _{2eq} /kg.	48
Figure 25: Share of CO _{2eq} emissions by mined potassium chloride from SQM, Chile. The overall GHG emissions are estimated to generate 0.48 kgCO _{2eq} /kg.	49
Figure 26: Share of CO _{2eq} emissions from the manufacturing process by mined solar salt at SQM, Chile. This process includes the crystallization from sodium nitrate and potassium chloride to the favorable mix of sodium nitrate (60 wt%) and potassium nitrate (40 wt%).	49
Figure 27: Share of CO _{2eq} emissions from the manufacturing process by EAF slag pebbles via the sintering process and via the mechanical conformation. The amount of estimated GHG emissions from the sintering process is more than double (0.64 kgCO _{2eq} /kg) compared to the mechanical conformation method (0.28 kgCO _{2eq} /kg). The illustration ratio between both methods is 1:1.	50
Figure 28: Comparison of the embodied life-cycle GHG emissions from materials used in indirect and direct two-tank and thermocline molten solar salt and air TES systems designed to supply 6 hours of thermal storage for 50 MWe CSP plants.	51
Figure 29: Comparison of the embodied GHG emissions from materials and energy used in the thermocline storage systems.	52
Figure 30: Share of CO _{2eq} emissions by thermal mass component from materials and energy used in the thermocline storage systems.	52
Figure 31: Life-cycle GHG emissions of the EAF slag-based thermocline TES storage. The functional unit represents a 1 GWht thermal storage capacity for a 50 MWe CSP central receiver plant located in Seville, Spain. A lifetime of 30 years and a yearly discharging rate of 340 are assumed.	53
Figure 32: LCIA results of the EAF slag-based thermocline TES storage based on the functional unit of 1 GWht with a lifetime of 30 years and a yearly discharging rate of 340. The indicators are based on the recommendation by Hauschild et al. (2013). The graphic shows the results based on a log ₁₀ scale.	54
Figure 33: Share of life-cycle GHG emissions by CSP tower components for a 50 MWe steam turbine incorporating a 6 hour direct TES system designs located in Seville, Spain. The functional unit is based on 1 kWhe of electricity production.	55
Figure 34: Selected life-cycle environmental impacts of current electricity generation systems in Spain (per kWhe). The CSP tower plant incorporates the EAF slag-based packed bed system design 2b (mechanical conformation). LCI data of the alternative technologies are selected from the Ecoinvent database 3.3 (Wernet, et al., 2016). The selected LCIA indicators are based on the recommendation by Hauschild et al. (2013). The graphic shows the results based on a log ₁₀ scale.	56

APPENDIX B: LIST OF TABLES

Table 1: Slagstock major Work Packages and participants; Coordinator: CIC energiGUNE. Further partner: University Erlangen / Nuremberg.	4
Table 2: Physical properties of selected thermal energy storage media. Sensible energy storage media, both liquid and solid, are assumed to have a storage temperature differential of 350°C with respect to the calculation of volumetric and gravimetric storage density (Siegel, 2012).	14
Table 3: Design configurations of the thermocline TES system for the application for HTF as air (system 1) and molten solar salt (system 2).	34
Table 4: Assumed densities of used bulk materials.	40
Table 5: Thermocline storage tank insulation and foundation – Design specifications	41
Table 6: Material inventory for the production of 1kg sintered EAF slag pebbles using several production steps: crushing, rolling, mixing, drying, and cooking.	43
Table 7: Material inventory for the production of 1kg mechanical conformed EAF slag pebbles via tumbling, washing, and air drying.	44
Table 8: Results of the design parameter simulation by SAM modelled for a 50 MWe CSP tower plant located in Seville, Spain.	45
Table 9: Siemens CSP turbine specifications. The SST-300 steam turbine is suitable for a 50 MWe CSP plant and requires a steam inlet pressure of 12 MPa and a temperature of 520°C (Siemens AG, 2010).	46
Table 10: Life-cycle GHG emissions for the EAF slag-based packed bed TES systems per electricity output from the stored thermal capacity.	53

APPENDIX C: LIST OF ABBREVIATIONS

CO _{2eq}	Carbon dioxide equivalent
CSP	Concentrated Solar Power
DNI	Direct Normal Irradiance (e.g. in kWh/m ² /a)
DSG	Direct Steam Generation
e	electric
EAF	Electric Arc Furnace
GHG	Greenhouse Gas
GWP	Global Warming Potential
HTF	Heat Transfer Fluid
IEA	International Energy Agency
ILCD	International Reference Life Cycle Data System
IPCC	Intergovernmental Panel on Climate Change
LCA	Life Cycle Assessment
LCI	Life Cycle Inventory
LCIA	Life Cycle Impact Assessment
LCOE	Levelised Cost of Electricity
NREL	National Renewable Energy Laboratory
PCM	Phase Change Material
PSI	Paul Scherrer Institute
PV	Photovoltaic
R&D	Research and Development
RT	Room Temperature
SAM	System Advisory Model
SSMT	Steam System Modeler Tool
STE	Solar Thermal Electricity
t	thermal
TES	Thermal Energy Storage
TWh	Terrawatt-hours
O&M	Operation and Maintenance

APPENDIX D: LCI DATACOLLECTION FOR TES SYSTEMS 1 – 5

Material inventory of the EAF slag based thermocline storage system for 50 MWe CPS central receiver plants – 1000 MWh / 6 hours packed bed with air as a HTF ([system 1](#)).

The following tables show the material inputs and outputs for the components:

- Thermocline storage tank (Table 1)
- Thermocline tank foundation (Table 2)
- Thermal mass (Table 3)
- Pumps and compressors (Table 4)

The material inventories of the EAF slag pebbles are listed in detail in chapter 5.3.

The material output refers to the end of life of the storage tank system and its consequential waste handling and disposal.

Table 1: Thermocline storage tank – Materials used and their purpose

Inputs	Amount	Unit	Comments
Chromium steel 18/8, hot rolled	135'676	kg	Used in the thermocline tank, the two surge tanks.
Rock wool	35'904	kg	Insulation material for the tanks.
Sand-lime brick	129'755	kg	Insulation material for the tanks.
Drawing of pipes, steel	120	kg	Process done to draw pipes from steel.
Wire drawing, copper	105	kg	The copper input is used to draw wires for field wiring, cables etc.
Copper	105	kg	Copper supplied for field wiring purposes.
Output	Amount	Unit	Comments
Treatment of waste reinforcement steel, recycling	73'265	kg	Today in the EU28 54% of all steel masses are recycled. The steel disposal measure followed for treatment of all feasible metallic components. In this case, reinforced steel is used as a proxy for unalloyed steel.
Treatment of waste reinforcement steel, collection for final disposal	62'411	kg	Today in the EU28 46% of all steel masses are sent for disposal. Disposal includes demolition, feeding into rubble containers and transport to landfill and landfill itself.
Treatment of waste mineral wool, collection for final disposal	35'904	kg	Rock wool used in insulation sent for final disposal.
Treatment of waste concrete, not reinforced, collection for final disposal	129'755	kg	Sand-lime bricks are sent to landfill.
Treatment of scrap copper, municipal incineration	105	kg	Scrap copper disposal

Table 2: Thermocline storage tank foundation – Materials used and their purpose

Inputs	Amount	Unit	Comments
Reinforcing steel	42'199	kg	Used in construction of tank foundation and impoundment wall.
Concrete	333	m ³	Concrete for elevated platform, impoundment wall, and to embed metals.
Foam glass	17'791	kg	Used in tank foundation insulation.
Refractory brick	44'729	kg	Used in tank perimeter foundation.
Excavation, hydraulic digger	447	m ²	Excavation and backfilling. The digger is a removable unit. All the soil dislocated for initial construction is put back. Hence no end of life calculation is needed.
Output	Amount	Unit	Comments
Treatment of waste reinforcement steel, recycling	22'787	kg	Today in the EU28 54% of all steel masses are recycled. The steel disposal measure followed for treatment of all feasible metallic components. In this case, reinforced steel is used as a proxy for unalloyed steel.
Treatment of waste reinforcement steel, collection for final disposal	19'411	kg	Today in the EU28 46% of all steel masses are sent for disposal. Disposal includes demolition, feeding into rubble containers and transport to landfill and landfill itself.
Treatment of waste concrete, not reinforced, collection for final disposal	778'149	kg	Sand-lime bricks are sent to landfill.
Treatment of waste glass, inert material landfill	17'791	kg	Inert material disposal

Table 3: Thermal mass – Materials used and their purpose

Inputs	Amount	Unit	Comments
EAF slag pebbles	5'991'553	kg	Used as a filler material in the thermocline tank.
Output	Amount	Unit	Comments
Treatment of inert waste, inert material landfill	5'991'553	kg	Nitrate salt inventory and EAF slag pebbles sent to landfill.

Table 4: Pumps and compressors – Materials used and their purpose

Inputs	Amount	Unit	Comments
Cast iron	6'214	kg	Used in the pumps and compressors.
Steel, low-alloyed, hot rolled	604	kg	Material composition in pumps and compressor.
Chromium steel 18/8	7'491	kg	Material composition in pumps and compressor.
Tap water	30'700	kg	Water used in the process of manufacturing of pumps.
Output	Amount	Unit	Comments
Treatment of waste reinforcement steel, recycling	7'730	kg	Today in the EU28 54% of all steel masses are recycled. The steel disposal measure followed for treatment of all feasible metallic components. In this case, reinforced steel is

Treatment of waste reinforcement steel, collection for final disposal	6'580	kg	used as a proxy for unalloyed steel. Today in the EU28 46% of all steel masses are sent for disposal. Disposal includes demolition, feeding into rubble containers and transport to landfill and landfill itself.
---	-------	----	--

Material inventory of the EAF slag based thermocline storage system for 50 MWe CPS central receiver plants – 1000 MWht / 6 hours packed bed with molten solar salt as a HTF ([system 2](#)).

The following tables show the material inputs and outputs for the components:

- Thermocline storage tank (Table 1)
- Thermocline tank foundation and impoundment wall (Table 2)
- Thermal mass (Table 3)
- Pumps and compressors (Table 4)

The material inventories of the EAF slag pebbles are listed in detail in chapter 5.3.

The material output refers to the end of life of the storage tank system and its consequential waste handling and disposal.

Table 1: Thermocline storage tank – Materials used and their purpose

Inputs	Amount	Unit	Comments
Chromium steel 18/8, hot rolled	216'265	kg	Used in the thermocline tank, the two surge tanks.
Reinforcing steel	9'583	kg	Used in the initial melting sump tank.
Rock wool	58'441	kg	Insulation material for the tanks.
Sand-lime brick	129'181	kg	Insulation material for the tanks.
Transformer, high voltage use	1'290	kg	Transformer setup including substation and primary power distribution sources.
Drawing of pipes, steel	120	kg	Process done to draw pipes from steel.
Wire drawing, copper	105	kg	The copper input is used to draw wires for field wiring, cables etc.
Copper	105	kg	Copper supplied for field wiring purposes.
Output	Amount	Unit	Comments
Treatment of waste reinforcement steel, recycling	121'958	kg	Today in the EU28 54% of all steel masses are recycled. The steel disposal measure followed for treatment of all feasible metallic components. In this case, reinforced steel is used as a proxy for unalloyed steel.
Treatment of waste reinforcement steel, collection for final disposal	103'890	kg	Today in the EU28 46% of all steel masses are sent for disposal. Disposal includes demolition, feeding into rubble containers and transport to landfill and landfill itself.
Treatment of waste mineral wool, collection for final disposal	58'441	kg	Rock wool used in insulation sent for final disposal.

Treatment of waste concrete, not reinforced, collection for final disposal	129'181	kg	Sand-lime bricks are sent to landfill.
Treatment of scrap copper, municipal incineration	105	kg	Scrap copper disposal

Table 2: Thermocline storage tank foundation and impoundment wall – Materials used and their purpose

Inputs	Amount	Unit	Comments
Reinforcing steel	27'559	kg	Used in construction of tank foundation and impoundment wall.
Concrete	268	m ³	Concrete for elevated platform, impoundment wall, and to embed metals.
Foam glass	7'299	kg	Used in tank foundation insulation.
Refractory brick	25'351	kg	Used in tank perimeter foundation.
Excavation, hydraulic digger	372	m ²	Excavation and backfilling. The digger is a removable unit. All the soil dislocated for initial construction is put back. Hence no end of life calculation is needed.
Output	Amount	Unit	Comments
Treatment of waste reinforcement steel, recycling	14'882	kg	Today in the EU28 54% of all steel masses are recycled. The steel disposal measure followed for treatment of all feasible metallic components. In this case, reinforced steel is used as a proxy for unalloyed steel.
Treatment of waste reinforcement steel, collection for final disposal	12'677	kg	Today in the EU28 46% of all steel masses are sent for disposal. Disposal includes demolition, feeding into rubble containers and transport to landfill and landfill itself.
Treatment of waste concrete, not reinforced, collection for final disposal	615'719	kg	Sand-lime bricks are sent to landfill.
Treatment of waste glass, inert material landfill	7'299	kg	Inert material disposal

Table 3: Thermal mass – Materials used and their purpose

Inputs	Amount	Unit	Comments
Solar salt	2'440'700	kg	Used as mined molten salt with 60 wt% sodium nitrate, and 40 wt% potassium nitrate contribution.
EAF slag pebbles	8'334'382	kg	Used as a filler material in the thermocline tank.
Heat, natural gas	140'000	MJ	Used to preheat the tank and filler material to prevent refreezing of the salt and thermal stresses to the tank of initial fill.
Electricity, medium voltage	554'000	kWh	Used to melt the salt before it is sent to the thermal storage tank, pumping power for tank feeding of initial fill. Auxiliary heat tracing efforts.
Output	Amount	Unit	Comments

Treatment of inert waste, inert material landfill	10'775'082	kg	Nitrate salt inventory and EAF slag pebbles sent to landfill.
---	------------	----	---

Table 4: Pumps and compressors – Materials used and their purpose

Inputs	Amount	Unit	Comments
Cast iron	561	kg	Used in the pumps and compressors.
Steel, low-alloyed, hot rolled	2'730	kg	Material composition in pumps and compressor.
Chromium steel 18/8	1'920	kg	Material composition in pumps and compressor.
Tap water	21'600	kg	Water used in the process of manufacturing of pumps.
Output	Amount	Unit	Comments
Treatment of waste reinforcement steel, recycling	2'810	kg	Today in the EU28 54% of all steel masses are recycled. The steel disposal measure followed for treatment of all feasible metallic components. In this case, reinforced steel is used as a proxy for unalloyed steel.
Treatment of waste reinforcement steel, collection for final disposal	2'400	kg	Today in the EU28 46% of all steel masses are sent for disposal. Disposal includes demolition, feeding into rubble containers and transport to landfill and landfill itself.

Material inventory of a two-tank TES system for 50 MWe CSP tower plant (system 3).

Thermal storage systems for CSP tower applications (Telsnig, 2015)	Direct two-tank TES system with molten salt		
	Output	Input	Unit
Ecoinvent process			
Reinforcing steel		194'152	kg
Steel, chromium steel 18/8, hot rolled		161'486	kg
Solar salt		7'091'965	kg
Heat, district or industrial, natural gas		2'717'799	MJ
Steel, low-alloyed		4'974	kg
Tin plated chromium steel sheet, 2 mm		18	m ²
Rock wool		111'636	kg
Transformer, high voltage use		1'290	kg
Drawing of pipes, steel		183	kg
Wire drawing, copper		116	kg
Copper		116	kg
Concrete, normal		655	m ³
Excavation, hydraulic digger		972	kg
Foam glass, at plant		22'942	kg
Refractory, basic, packed, at plant		81'229	kg
Sand		22'817	kg

Alkyd paint, white, without solvent, in 60% solution state	170	kg
Treatment of waste paint, inert material landfill	170	kg
Treatment of waste reinforcement steel, recycling	126'214	kg
Treatment of waste reinforcement steel, collection for final disposal	194'730	kg
Treatment of waste concrete, not reinforced, collection for final disposal	197'670	kg
Treatment of inert waste, inert material landfill	7'091'965	kg
Treatment of scrap copper, municipal incineration	116	kg
Treatment of waste glass, inert material landfill	22'942	kg
Treatment of waste mineral wool, collection for final disposal	111'636	kg

Material inventory of thermocline TES system for 50 MWe CSP plant (system 4).

Thermal storage systems for CSP trough applications (Heath, Turchi, Burkhardt, Kutscher, & Decker, 2009)		Indirect thermocline with quartzite rock, sand & molten salt (6 hours)		
LCI	Ecoinvent process	Output	Input	Unit
Thermal Mass				
Molten solar salt	Mined solar salt		7'680'000	kg
Quartzite rock and sand	Silica sand		17'900'000	kg
Heat, natural gas	Heat, industrial, NG		2'943'146	MJ
Inert waste		25'580'000		kg
Storage Tank				
Carbon steel	Reinforcing steel		456'000	kg
Stainless steel	Chromium steel 18/8 hot rolled		3'080	kg
Mineral wool	Rock wool		158'000	kg
Calcium silicate	Sand-lime brick		25'700	kg
Transformer, high voltage use			1'290	kg
Waste concrete		25'700		kg
Waste mineral wool		158'000		kg
Waste reinforced steel recycling		247'903		kg
Waste reinforced steel landfill		211'177		kg
Storage Tank Foundation + Platform+ impoundment wall				
Carbon steel	Reinforcing steel		231'000	kg
Concrete			527	m3
Foam glass			44'000	kg
refractory brick	Refractory basic		432'000	kg
Waste concrete		3791'400		kg
Waste glass		44'000		kg
Waste reinforced steel recycling		177'120		kg
Waste reinforced steel landfill		150'880		kg

Storage Nitrogen system			
Calcium silicate	Sand-lime brick	2'460	kg
Carbon steel	Reinforcing steel	17'900	kg
Nitrogen	Nitrogen liquid	28'100	kg
Waste reinforced steel recycling		9'666	kg
Waste reinforced steel landfill		8'234	kg
Waste concrete		2'460	kg
Heat exchanger			
Calcium silicate	Sand-lime brick	38'900	kg
Stainless steel	Chromium	179'000	kg
Waste reinforced steel recycling		96'660	kg
Waste reinforced steel landfill		82'340	kg
Waste concrete		38'900	kg

**Material inventory of thermocline TES system for 50 MWe CSP trough plant.
(system 5)**

Thermal storage systems for CSP trough applications (Telsnig, 2015)	Indirect two-tank TES system with molten salt		Unit
	Output	Input	
Ecoinvent process			
Reinforcing steel		2565829	kg
Cast iron		29937	kg
Low alloyed steel		28253	kg
Silicone product		7181	kg
Chromium steel 18/8, hot rolled		57345	kg
Particle board, cement bonded		1	m ²
Tap water		105484	kg
Rock wool		139920	kg
Sheet rolling, chromium		51	kg
Sheet rolling, steel		287	kg
Aluminium, cast alloy		50	kg
Sheet rolling, aluminium		50	kg
Copper		9831	kg
Wire drawing copper		9831	kg
Synthetic rubber		3	kg
Polystyrene, high impact		8	kg
Injection moulding		8	kg
Glass fibre		9	kg
Polyethylene, high density, granulate		18	kg
Extrusion, plastic pipes		18	kg
Tin plated chromium steel sheet, 2 mm		100	m ²
Drawing of pipe, steel		221738	kg

Welding arc, steel	1010	kg
Transformer, high voltage use	17389	kg
Control cabinet cogen unit, 160kW electrical	3	parts
Iron-nickel-chromium alloy	41753	kg
Concrete, normal	1734	m3
Excavation, hydraulic digger	4067	kg
Foam glass, electricity, label-certified	121704	kg
Refractory, basic, packed	409230	kg
Sand, at mine	93967	kg
Alkyd paint, white, without solvent, in 60% solution state	1204	kg
Solar salt	17759294	kg
Expanded perlite	558872	kg
Heat, district or industrial, natural gas	11342926	MJ
Waste paint	1204	kg
Scrap aluminium	50	kg
Treatment of waste reinforcement steel, recycling	953091	kg
Treatment of waste reinforcement steel, collection for final disposal	1770026	kg
Waste concrete	4783259	kg
Waste glass	121713	kg
Inert waste	29598824	kg
Scrap copper	9831	kg
Waste mineral wool	139920	kg
Waste polyethylene	18	kg
Waste rubber, unspecified	3	kg
Waste polystyrene	8	kg

APPENDIX E: LCI DATA COLLECTION FOR CSP COMPONENTS

Material inventory for additional components of a 50 MW CSP tower plant in Seville, Spain.

CSP tower plant, 50 MWe steam turbine located in Seville, Spain			
Ecoinvent process	Output	Input	Unit
Infrastructure			
Road		53049	m*a
Wire drawing, steel		4563	kg
Steel, unalloyed		4563	kg
Excavation, hydraulic digger		22937	m3
Water supply network		5	km
Building, hall, steel construction		2411	m ²
Transformation, from grassland, natural (non-use)		1569475	m ²
Transformation, to industrial area		1569475	m ²
Occupation, industrial area		47084261	m ² *a
Decommissioned road	53049		m*a
Treatment of waste reinforcement steel, recycling	2464		kg
Treatment of waste reinforcement steel, collection for final disposal	2099		kg
Collector field area construction, solar tower, 50 MW	1		unit
Receiver system for a solar tower plant, 50MW	1		unit
Thermal storage system, solar tower, 50 MW	1		unit
Steam generation system for solar tower plant, 50MW	1		unit
Power block, for 50MW solar tower plant	1		unit
Solar field			
Reinforcing steel		12316585	kg
Cast iron		2068161	kg
Flat glass, coated		4549953	kg
Concrete, normal		5810	m3
Welding, arc, steel		60794	kg
Wire drawing, copper		62132	kg
Copper		62241	kg
Treatment of waste reinforcement steel, recycling	7767763		kg
Treatment of waste reinforcement steel, collection for final disposal	6616983		kg
Scrap copper	62241		kg
Waste concrete	12781993		kg
Waste glass	4549953		kg
Receiver system			
Cast iron		40042	kg
Silicon product		2397	kg
Particle board, cement bonded		304	m ²
Tap water		27727	kg

Steel, chromium steel 18/8, hot rolled	4417	kg
Iron nickel chromium alloy	545810	kg
Metal working, average for metal product manufacturing	62564	kg
Reinforcing steel	2303408	kg
Drawing of pipe, steel	1290941	kg
Welding, arc, steel	5098	m
Steel, low-alloyed	12522	kg
Tin plated chromium steel sheet, 2 mm	35	m ²
Expanded perlite	868761	kg
Transformer, high voltage use	2363	kg
Wire drawing, copper	891	kg
copper	891	kg
Concrete, normal	5278	m ³
Excavation, hydraulic digger	3473	m ³
Hazardous waste, for incineration	585	kg
Municipal solid waste	202	kg
Treatment of waste reinforcement steel, recycling	1569347	kg
treatment of waste reinforcement steel, collection for final disposal	1336851	kg
Waste concrete	12479715	kg
Treatment of scrap copper, municipal incineration	891	kg
Steam generation system		
Reinforcing steel	294094	kg
Cast iron	4803	kg
Silicon product	14	kg
Steel, low-alloyed	2727	kg
Tap water	21623	kg
Steel, chromium steel 18/8, hot rolled	1920	kg
Drawing of pipes, steel	35561	kg
Welding, arc, steel	170	m
Expanded perlite	59220	kg
Transformer, high voltage use	131	kg
Iron-nickel-chromium alloy	22135	kg
Wire drawing, copper	200	kg
Copper, at regional storage	200	kg
Concrete, normal	17	m ³
Excavation, hydraulic digger	13	m ³
Alkyd paint, white, without solvent, in 60% solution state	63	kg
Hazardous waste, for incineration	76	kg
Municipal solid waste	120	kg
Waste paint	63	kg
Treatment of waste reinforcement steel, recycling	175867	kg
Treatment of waste reinforcement steel, collection for final disposal	149812	kg
Waste concrete	96109	kg
Scrap copper	200	kg

Power block		
Aluminium alloy, metal matrix composition	500483	kg
Reinforcing steel	2318072	kg
steel, low-alloyed	389465	kg
Glass fibre reinforced plastic	482123	kg
Cast iron	104510	kg
Zinc	1213	kg
Concrete, normal	17494	m ³
Section bar rolling, steel	301165	kg
Zinc coating, coils	19275	m ²
Drawing of pipe, steel	1869195	kg
Metal working, average for aluminium product manufacturing	500373	kg
Silicon product	13917	kg
Particle board, cement bonded	203	m ³
Tap water	40400	kg
Steel, chromium steel 18/8, hot rolled	22363	kg
Aluminium, cast alloy	101	kg
Sheet rolling, aluminium	101	kg
Sheet rolling, chromium steel	102	kg
Sheet rolling, steel	589	kg
Wire drawing copper	8497	kg
Synthetic rubber production	7	kg
Copper, supply mix	16577	kg
Polystyrene, high impact	17	kg
Injection moulding	17	kg
Molybdenum	907	kg
Iron-nickel-chromium alloy	36332	kg
Steel milling, average	38916	kg
Chromium steel milling, average	12586	kg
Cast iron milling, average	11833	kg
Ceramic plate	3900	kg
Polyethylene, high density granulate	2200	kg
Extrusion, plastic pipes	526	kg
Welding arc, steel	977	m
Expanded perlite	174241	kg
Glass fibre production	1006	kg
Kraft paper, unbleached	368	kg
Alkyd paint, white, without solvent, in 60% solution state	381	kg
Brass	5	kg
Electricity, high voltage	402840	kWh
Heat, district or industrial, other than natural gas	142118	MJ
Transformer, high voltage use	567	kg
Excavation, hydraulic digger	751	m ³
Polyvinylchloride	8	kg
Sand	95	kg
Hazardous waste, for incineration	602673	kg

Appendix E: LCI datacollection for CSP components

Municipal solid waste	1823117	kg
Waste paint	381	kg
Treatment of waste reinforcement steel, recycling	1551347	kg
Treatment of waste reinforcement steel, collection for final disposal	1321518	kg
Waste concrete	39111686	kg
Scrap copper	16577	kg
Waste glass	1006	kg
Scrap aluminum	500583	kg
Waste polyethylene/polypropylene product	484330	kg
Waste rubber, unspecified	7	kg
Waste polystyrene	17	kg

APPENDIX F: CSP SCALING FUNCTIONS

Listing of scaling functions are established by Telsnig (2015)

The material inventory are based on a hypothetical reference system design engineered by Abengoa Solar (Kelly B. , 2010) and scaled down from a 440 MWe CSP tower reference plant to the evaluated 50 MWe CSP tower plant.

Formula directory:

Collector field area	A_{SF}
Thermal heat storage capacity	Q_{TS}
Thermal heat storage capacity single pair of tanks	Q_{TStank}
Electrical power output	P_e
Steam mass flow rate	m_S
Steam turbine power	P_{ST}

Specific construction work	Scaling function
I - Infrastructure	
Site Improvements	$f_{Si} = A_{SF}/A_{SF(ref)}$
Piping (water supply)	$f_{PT} = 1$
Buildings	$f_B = 1$
II - Collector system	
Collector field	$f_{CF} = 1/n (A_{SF}/A_{SF(ref)})$, n: Solar field amount
Pumps	
Compressors	
Special equipment	
Valves	
Structural Steel	$f_{CF2} = (m_S/m_{S(ref)})$
Electrical	
Concrete work	
Site work	
Paint	
Piping	
Insulation	$f_{CF3} = (m_S/m_{S(ref)})^{(1/2)}$
III - Receiver system	
Receiver	
Piping	$f_{RS_1} = 1/n (m_S/m_{S(ref)})^{(1/2)}$,
Insulation	n: Receiver amount
Pumps	
Instrumentation	$f_{RS_2} = A_{SF}/A_{SF(ref)}$

Structural Steel	
Electrical	
Concrete work	
Site work	
IV - Thermal storage system	
Columns and Vessels	$f_{TS(n)} = 1/n(Q_{TS_Tank} / Q_{TS_Tank(ref)}), n: \text{Tank amount}$
Storage Tanks	
Pumps	
Valves	$f_{TS(1)} = (Q_{TS}/Q_{TS(ref)})^{(2/3)}$
Insulation	
Painting	
Compressors	
Molten Salt	
Instrumentation	
Structural Steel	$f_{TS} = (Q_{TS}/Q_{TS(ref)})$
Electrical	
Concrete work	
Site work	
Piping	
	$f_{TS_PT} = (m_S/m_{S(ref)})^{(1/2)}$
V - Steam generation	
Pumps	
Valves	
Electrical	$f_{SG1} = P_e/P_{e(ref)}$
Concrete work	
Site work	
Paint	
Heat exchanger	
Piping	$f_{SG2} = (m_S/m_{S(ref)})^{(1/2)}$
Insulation	
VI - Power block	
Columns & Vessels	
Tanks	
Pumps	
Compressors	$f_{PB1} = P_e/P_{e(ref)}$
Structural Steel	
Electrical (Transformer)	
Electrical (Bulk Material)	
Concrete work	

Site work	
Piping	
Insulation	$f_{PB2} = (m_S/m_{S(ref)})^{(1/2)}$
Heat Exchangers	
Cooling tower	$f_{CT} = (m_S/m_{S(ref)})^{(1/2)}$
Steam Turbine	
Generator	$f_{PB3} = (P_{ST}/P_{ST(ref)})^{(1/2)}$
Cranes(EPGS)	$f = 1$

APPENDIX G: LCI DATACOLLECTION SOLAR SALT

Material inventory for the SQM solar salt production, Chile.

Solar salt SQM (2017)	per 1kg production		Unit
	Output	Input	
Ecoinvent process			
Caliche ore			
Transformation, from unknown		1.4E-07	m ²
Transformation, to mineral extraction site		1.4E-07	m ²
Occupation, mineral extraction site		1.4E-07	m ² a
Diesel burned in Machines		0.023	kg
Electricity		0.014	kWh
Transport, freight, lorry		3	kg
Transport, freight, train		31	kg
Sodium nitrate			
Caliche ore		1.580	kg
Heat, natural gas		0.580	MJ
Tap water		2.400	kg
Transport, freight, lorry		23.000	kg
Particles, unspecified	8.0E-09		kg
Inert waste	0.574		kg
Potassium chloride			
Water, salt, sole	in ground	0.027	m ³
Transformation, from unknown	land	1.4E-05	m ²
Transformation, to mineral extraction site	land	1.4E-05	m ²
Occupation, mineral extraction site	land	3.7E-02	m ² a
Polyvinylfluoride, film		0.019	kg
Diesel burned in machines		0.009	MJ
Electricity		0.084	kWh
Transport		180	km
Solar salt			
Sodium nitrate		1.269	kg
Potassium chloride		0.988	kg
Heat, natural gas		0.330	MJ
Electricity		0.148	kWh
Tap water		1.056	kg
Transport, freight, lorry		230	km
Transport, freight, sea, transoceanic ship		12768	km

APPENDIX H: DECLARATION / ERKLÄRUNG

Hiermit erkläre ich, dass ich die vorliegende Arbeit selbständig verfasst und keine anderen als die angegebenen Hilfsmittel und Quellen verwendet habe.

Basel, 30 October 2017

(Unterschrift)

Mit der Weitergabe meiner Master Thesis durch die Universität Koblenz – Landau an Dritte (z.B. Bibliotheken, Behörden, Unternehmen, interessierte Privatpersonen) erkläre ich mich einverstanden.

Basel, 30 October 2017

(Unterschrift)